A Sober Look at the Robustness of CLIPs to Spurious Features

Qizhou Wang[1*] **Yong Lin**[2*] **Yongqiang Chen**[3*]
Ludwig Schmidt[4] **Bo Han**[1†] **Tong Zhang**[5]

[1]TMLR Group, Department of Computer Science, Hong Kong Baptist University
[2]The Hong Kong University of Science and Technology
[3]The Chinese University of Hong Kong
[4]University of Washington
[5]University of Illinois Urbana-Champaign

https://counteranimal.github.io/

Abstract

Large vision language models, such as CLIP, demonstrate impressive robustness to spurious features than single-modal models trained on ImageNet. However, existing test datasets are typically curated based on ImageNet-trained models, which aim to capture the spurious features inherited in ImageNet. Benchmarking CLIP models based on the ImageNet-oriented spurious features may not be sufficient to reflect the extent to which CLIP models are robust to spurious correlations within CLIP training data, e.g., LAION. To this end, we craft a new challenging dataset named `CounterAnimal` designed to reveal the reliance of CLIP models on realistic spurious features. Specifically, we split animal photos into groups according to the backgrounds, and then identify a pair of groups for each class where a CLIP model shows high-performance drops across the two groups. Our evaluations show that the spurious features captured by `CounterAnimal` are generically learned by CLIP models with different backbones and pre-train data, yet have limited influence for ImageNet models. We provide theoretical insights that the CLIP objective cannot offer additional robustness. Furthermore, we also re-evaluate strategies such as scaling up parameters and high-quality pre-trained data. We find that they still help mitigate the spurious features, providing a promising path for future developments.

1 Introduction

Large vision language models (LVLMs) have demonstrated huge success across a wide range of vision and multi-modal tasks, surpassing conventional ImageNet (-trained) models by a remarkably large margin [1]. LVLMs are typically trained with or based on Contrastive Language Image Pre-training (CLIP) [2] on an unprecedented scale of real-world vision and language data such as LAION [3], which are significantly larger than ImageNet. The huge success of CLIP has presented a paradigm shift for modern vision and vision-language models to conduct the pre-training from ImageNet benchmarks to web-scale multi-modal datasets [4].

A key signature of CLIP models is the impressive robustness against various ImageNet-oriented distribution shifts [2], which is shown to be prohibitive to ImageNet models [5]. The performance

[*] Equal contributions.
[†] Correspondence to Bo Han (bhanml@comp.hkbu.edu.hk).

38th Conference on Neural Information Processing Systems (NeurIPS 2024).

https://doi.org/10.52202/079017-3893

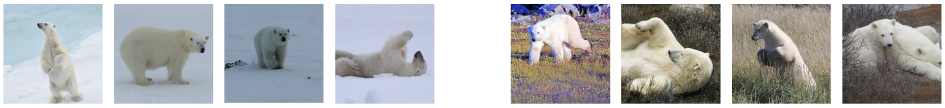

Photos of **ice bear** in **snow** background (**easy**, accu 97.62)

Photos of **ice bear** in **grass** background (**hard**, accu 70.91)

Figure 1: We showcase `CounterAnimal` examples from the class of `ice bear`, separated into `easy` and `hard` groups with different backgrounds (i.e., `snow` and `grass`). The zero-shot performance of `CLIP-LAION400M-ViT-B/32` drops from 97.62% (`easy`) to 70.91% (`hard`).

boosts over ImageNet models seem to suggest that CLIP resolves distribution shifts, thereby sparking a rich discussion about its rationale [6, 7, 8, 9, 10]. However, *the elephant in the room* is that adopted testsets (i.e., ImageNet variants) to evaluate the robustness of CLIPs are primarily designed for ImageNet-based models [5, 11]. These datasets may not correctly reflect the exact robustness of CLIP, given that CLIP models are trained on a large amount of data that may include, and possibly extend beyond those ImageNet variants during pre-training [10]. In this paper, we investigate the robustness of CLIP to distribution shifts caused by the presence of spurious features. These features are highly correlated with labels, but this correlation may break down under distributional shifts [12, 13, 14, 15, 16, 17, 18, 19, 20]. We raise a challenging research question in the following:

Is there a benchmark that reflects the exact reliance on spurious features of CLIP?

Sadly, most of the existing benchmarks [21, 22, 23, 24] are tailored primarily for ImageNet models, which are unsuitable for CLIP. To fill this gap, we introduce a new testset, named `CounterAnimal`, specifically designed for assessing the robustness of CLIP models against real-world spurious features. Figure 1 presents several examples of `CounterAnimal` where data are divided into two groups, a) the `easy` group: animals in commonly appeared backgrounds that the CLIP models make correct predictions, and b) the `hard` group: animals in less commonly yet still plausible backgrounds, where the CLIP models are likely to misclassify them. Intuitively, the `easy` part captures some real-world biases that the web-scale data may naturally inherit. Hence, by comparing the performances of the two groups, one can quantify to what extent the model relies on spurious features.

Table 1: 1 vs. 1000 results of exemplary animal classes within the `CounterAnmial` dataset for `CLIP-LAION400M-ViT-B/32`. "bkg" denotes the background label, "accu" (%) denotes the zero-shot accuracy, and "drop" (%) denotes the drop in accuracy between `easy` and `hard` groups.

object label	`easy`		`hard`		drop
	bkg	accu	bkg	accu	
`ice bear`	`snow`	97.62	`grass`	70.91	26.71
`black swan`	`water`	93.63	`earth`	68.87	24.76
`flamingo`	`water`	79.70	`sky`	55.45	24.25
`vulture`	`sky`	87.76	`tree`	41.84	45.92
`dung beetle`	`earth`	56.92	`hand`	17.02	39.90

More specifically, the `CounterAnmial` dataset is curated based on raw photos collected from iNaturalist[3]. The construction pipeline consists of 4 steps. a) Data collection: querying iNaturalist with each animal class, where we select some of the animal names from the ImageNet-1K dataset [25]. b) Data curation: manually cleansing low-quality photos that potentially contain ambiguity and corruption. c) Background labeling: manually annotating photos with their respective backgrounds, selected from the label space of the candidate backgrounds. d) Spurious discovering: preserving classes and associated data based on the decrease in zero-shot performance (i.e., evaluating based on pre-trained CLIP models without fine-tuning) when shifting the backgrounds. The resulting `CounterAnimal` dataset covers a total of 45 animal classes, and ends up with 7,174 `easy` photos and 5,926 `hard` photos, aligning with the standard size as an evaluation dataset, such as [26, 27]. Moreover, `CLIP-LAION400M-ViT-B/32` is used as the proxy CLIP model in spurious discovering (cf., Appendix C.5 for the model naming rules).

We evaluate the CLIP models on our `CounterAnmial` with various backbones, e.g., ViT [28], along with different pre-train datasets, e.g., LAION [3]. We also consider more advanced LVLMs like MiniGPT4 [29] and LLaVA [30]. We employ two evaluation setups crafted for different families of models (cf., Appendix C): a) **1 vs. 1000 setup**: using the full ImageNet-1K class names as the candidate label space and b) **1 vs. 20 setup**: using the top-20 most confusing classes regarding `CLIP-LAION400M-ViT-B/32` as the candidate label space. We provide some of results in Table 1 and Figure 2, highlighting the key observations in the following:

[3] `https://www.inaturalist.org/observations`

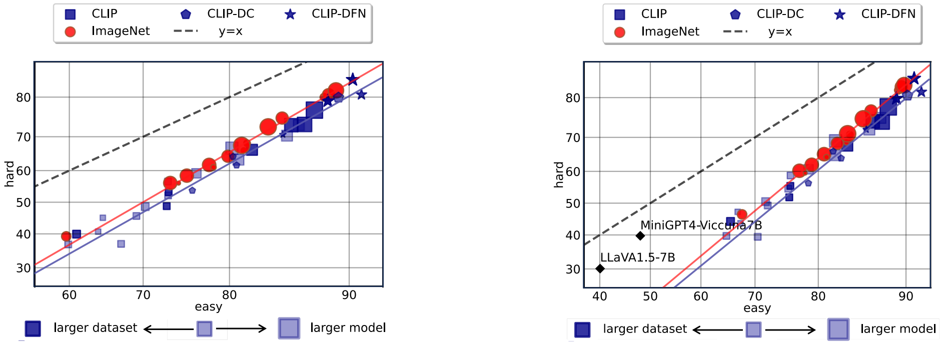

(a) **1 vs. 1000** (label space of ImageNet-1K)

(b) **1 vs. 20** (20 most confusing labels per class)

Figure 2: The `easy` vs. `hard` performance (%) for CLIP, ImageNet models, and more advanced LVLMs, i.e., MiniGPT4 and LLaVA. The marker size indicates the backbone scale and the color shade indicates pre-train data scale. We highlight the CLIP models pre-trained on high-quality datasets, i.e., DataComp (CLIP-DC) and Data Filtering Networks (CLIP-DFN). We linearly fit the trends for CLIP (CLIP, CLIP-DC, and CLIP-DFN) and ImageNet models to show their effective robustness. We also depict the perfect trend, i.e., $y = x$, where the models will not learn any bias.

`CounterAnimal` captures general spurious correlations within CLIP. As exemplified in Table 1, we observe a significant drop of `CLIP-LAION400M-ViT-B/32` in zero-shot accuracy from the `easy` to `hard` groups for each class. Furthermore, the observed biases in `CLIP-LAION400M-ViT-B/32` also generalize to other CLIP configurations, with non-trivial performance drop from the `easy` to `hard` groups across various backbones and pre-train datasets as in Figure 2. It implies that `CounterAnimal` characterizes some general spuriousness common in large-scale multi-modal datasets.

ImageNet models are more robust to spurious correlations captured by `CounterAnimal`. Figure 2 also illustrates the performance changes of ImageNet models (colored in red). Compared with CLIP models (colored in blue), we find that ImageNet models exhibit stronger robustness to spurious correlations captured by `CounterAnimal`. Our findings contrast with previous studies that assess the ImageNet variants [2], highlighting that CLIP models do not always generalize better than ImageNet models. It underscores the necessity of choosing appropriate benchmarks to comprehensively assess the robustness of different models and training schemes.

Larger CLIP models are more robust. Shown also in Figure 2, we use the sizes and the color shades of the markers to indicate the scales of backbones and the pre-train datasets, respectively. Overall, larger CLIP backbone models (i.e., larger markers) can improve the effective robustness, implying that scaling up backbones may enhance model performance against spurious features. In contrast, increasing the scale of the pre-train dataset (i.e., darker markers) does not yield the same improvement, implying that collecting more data alone cannot rectify much bias, which provides some new understanding in addition to the data-centric perspective [6, 10].

CLIP models trained on high-quality data are more robust. We categorize CLIP models into two distinct groups according to the pre-train data quality: a) CLIP-DC using DataComp [4] and CLIP-DFN employing Data Filtering Networks [31], as well as b) those pre-trained on datasets that lack stringent curation, labeled simply as CLIP. The results indicate that CLIP models pre-trained on high-quality datasets demonstrate enhanced robustness in general. It suggests that enhancing data quality remains a promising strategy for mitigating the spurious features.

The CLIP objective may not offer additional robustness. Complementary to our empirical observations, we also provide theoretical explanations for the reasons why CLIP learns spurious features. We further conduct confirmatory experiments that fine-tune CLIP models onto datasets with synthetic spurious features. The results align with our observations on `CounterAnimal` that the CLIP objective can not offer additional robustness over standard single-modal supervised training.

Comparison with previous results. Our work presents a new benchmark to effectively and systematically evaluate the robustness of CLIP models, which complements the literature in understanding the generalizability of CLIP models and LVLMs. More specifically, [32] reports that CLIP models

https://doi.org/10.52202/079017-3893

may wrongly align co-occurred objects with their texts. [33] reports similar failure modes for more sophisticated LVLMs such as MiniGPT4 or LLaVA. [34] finds that CLIP misaligned samples will further cause the hallucination of LVLMs. Complementary to these works, our study explicitly characterizes the spurious features captured by CLIP and explains the existence of the reported failure cases. Our study provides interesting empirical and theoretical counterexamples to the previous beliefs for the substantial improvements in robustness for CLIP models, especially for those results observed on ImageNet variants [7, 8, 9, 35]. Based on the newly collected `CounterAnimal` dataset, we suggest that distribution shifts remain an open problem for CLIP models. Also, we need to be cautious about the test setups when evaluating new models pre-trained on datasets that differ significantly in scales and distributions from traditional ImageNet models.

Comparison with previous benchmarks. There are many other datasets to study distribution shifts, e.g., ImageNet variants [21, 26, 36, 37, 38, 39, 40], `DomainBed` [41], and `Wilds` [42]. However, these datasets have biases when assessing the OOD robustness of CLIP models, as they may fail to represent the true OOD scenarios during CLIP training. Moreover, numerous recently released datasets, such as [22, 23, 43, 44, 45], have also explored distribution shifts. However, these studies primarily focus on synthetic distribution shifts, which may not fully represent real-world cases. In fact, it has been shown that previous OOD benchmarks are contained in CLIP training [10], making it hard to ablate ID/OOD cases for data in these benchmarks. Consequently, CLIP models have shown to be more robust than ImageNet models on these contaminated datasets [46].

2 Dataset and Evaluation Setups

To begin with, we describe the basic experimental setups, including the pipelines in constructing `CounterAnimal`, its key characteristics, as well as the adopted evaluation settings.

2.1 Construction of `CounterAnimal`

We introduce the curation pipeline of our new dataset `CounterAnimal`, tailored for CLIP to investigate spurious correlations. The pipeline consists of 4 steps as follows:

Data Collection. We query animal names listed in the ImageNet-1K dataset and collect raw data via the search interface of iNaturalist, a global biodiversity data-sharing platform. We retrieve the latest 300-800 photos per animal class, organizing them based on the queried labels.

Data Curation. The collected raw samples are susceptible to noise and ambiguities. Therefore, we manually cleanse the low-quality data that fall into any one of the following 4 situations: label noise, feature noise, obscurity, and clarity. Label noise refers to cases where photos do not belong to the queried classes; feature noise refers to cases where some pixels are disrupted or missing; obscurity occurs when photos belong to more than one object class; clarity issues refer to cases where animal objects are largely occluded by the backgrounds or other irrelevant objects. It also includes the cases where animal objects do not occupy the majority of the space in photos.

Background labeling. We consider a typical form of spurious features where the backgrounds of photos can be biased [47]. To identify such data for CLIP models, we manually label the backgrounds for the curated data. The considered class space of backgrounds is defined as follows: `ground, water, earth, sand, snow, grass, human, sky, road, rock, shrub, indoor, tree,` and `outdoor.` Note that the class space of backgrounds as above is not entirely orthogonal due to the inherent ambiguity: Some backgrounds may be ambiguous and some photos may contain more than one background. Nevertheless, we try our best to determine the assigned background labels for each animal class and exclude those photos challenging to be labeled.

Spurious Discovery. For each class, we quantify the impacts of spurious correlations to CLIP models by comparing the performances on the associated samples across different backgrounds. We take those classes as containing spurious features on which we observe a relatively obvious decrease in accuracy when changing backgrounds. In realization, we adopt the checkpoint of `CLIP-LAION400M-ViT-B/32` for evaluation, where the prompt for its text encoder is "`A photo of <object label>.`", and the space of `<object label>` is the ImageNet-1K class names, i.e., we follow an 1 vs. 1000 setup. Then, we consider the classes where the zero-shot accuracy varies by more than 5% when changing backgrounds as the cases where CLIP model has learned the spurious features. The data with the preserved classes and backgrounds are used to create our final

https://doi.org/10.52202/079017-3893

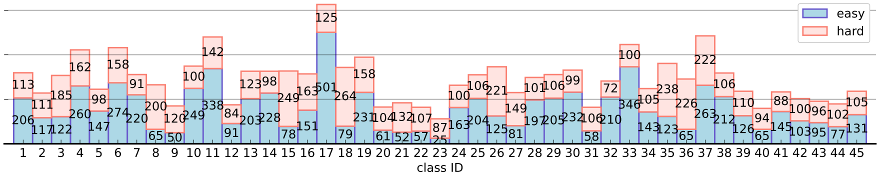

Figure 3: The data layout across various animal classes. The horizontal axis denotes the class IDs and the vertical axis denotes the number of photos for the easy and hard groups, respectively.

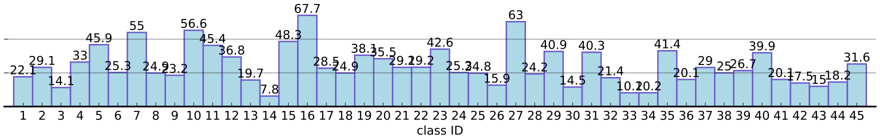

Figure 4: The 1 vs. 1000 performance drop (%) with CLIP-LAION400M-ViT-B/32. The horizontal axis denotes the class IDs and the vertical axis denotes the percentage points of decline.

CounterAnimal dataset. Photos with the highest CLIP accuracy are assigned to the easy group, and those with the lowest CLIP accuracy are assigned to the hard group. We further refine the collected data to remove any mistake that the labelers may made during data curation and background labeling.

Our objective in developing CounterAnimal is to reflect the spurious correlations learned by CLIP. Therefore, we need to employ the CLIP models for dataset curation and thus ensure the construction is effectively biased towards CLIP configurations [26]. In Appendix E, we further show that our data curation pipeline is general and reliable to characterize the spurious features within the considered models. Moreover, our experimental results later in Section 3 will corroborate that the spurious features captured by our CounterAnimal dataset are general across different CLIP setups and may not be so influential for ImageNet benchmarks. These findings will justify that our crafted testset satisfies our primary objective in characterizing the spuriousness for CLIP specifically.

2.2 Characteristics of CounterAnimal

We depict the data layout in Figure 3 and visualize the zero-shot gaps for each animal class in Figure 4, where we use CLIP-LAION400M-ViT-B/32 as our referred model. Please refer to the detailed object/background names concerning the easy and hard groups in Appendix B. Recalling that, when CLIP models resort to the shortcut of data, the model performance will heavily correlate with the backgrounds presented in the easy group yet is compromised when coming to the hard group. Accordingly, Figure 4 implies a reliance for the CLIP models on the backgrounds.

2.3 Evaluation Setups

We evaluate a series of CLIP models on the CounterAnimal dataset for their zero-shot performance. For each class, we use the pre-defined prompt of "A photo of <object label>." as in our data collection procedure and the similarity between image and text embeddings in classification. By default, we use the label space of the ImageNet-1K dataset and report the top-1 accuracy, i.e., the 1 vs. 1000 setup. Moreover, when involving more advanced LVLMs, we adopt the 1 vs. 20 setup where we employ the top-20 most confusing classes regarding CLIP-LAION400M-ViT-B/32 as the candidate label space. For re-productivity, we adopt the pre-trained CLIP checkpoints from OpenCLIP [48] and ImageNet model checkpoints from the PyTorch repository. The model naming rules are in Appendix C.5 and the evaluation details are discussed in Appendix C.

3 Experimental Analysis

Our experiments center on the evaluation and the analysis of our CounterAnimal dataset. In Section 3.1, we examine the generality of the captured spurious correlations. In Section 3.2, we explore the potential facets that affect the robustness of CLIP models. In Section 3.3, we extend the evaluation to a broader family of models with different training paradigms.

https://doi.org/10.52202/079017-3893

3.1 Generality of the Spurious Correlations

In Section 2.1, we discover spurious correlations using CLIP-LAION400M-ViT-B/32 and collect associated data to build the CounterAnimal dataset. A critical problem then arises: Is our dataset a general benchmark to examine spurious correlations of CLIP with other pre-train datasets and backbones? Hence, we need to examine whether the biases in the CounterAnimal dataset can hinder the robustness of other CLIP models, where we consider two situations: a) fixing pre-train datasets while varying backbones and b) varying pre-train datasets while fixing backbones.

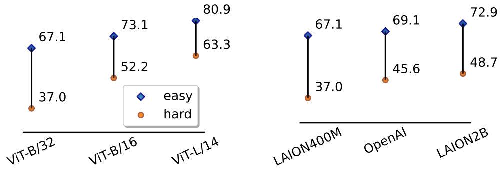

(a) LAION400M (b) ViT-B/32

Figure 5: The 1 vs. 1000 results for varying CLIP setups beyond CLIP-LAION400M-ViT-B/32: a) fixing the pre-train dataset to be LAION400M and b) fixing the backbone to be ViT-B/32.

Varying Backbones. We fix the pre-train dataset to be LAION400M and explore two other backbones within the ViT family [28], i.e., ViT-B/16 and ViT-L/14. Their zero-shot results are depicted in Figure 5(a). There remains a drop above 17 percentage points for both the cases of ViT-B/16 and ViT-L/14. It suggests that the CounterAnimal dataset captures some general spurious shifts that are at least present in the pre-train dataset of LAION400M.

Varying Pre-train Datasets. We fix the backbone to be ViT-B/32 and consider other pre-train datasets. Here, we consider LAION2B and the closed-source dataset used by OpenAI. Their easy and hard results are in Figure 5(b). Here, the spurious features affect the zero-shot robustness of CLIP models trained on both LAION2B and by OpenAI, indicating that our CounterAnimal dataset possesses some realistic shifts that are contained in various CLIP setups. Therefore, we conclude that CounterAnimal captures some general spurious features learned by CLIP models.

3.2 Scaling up May Relieve Spurious Correlations

We extend our evaluations to a wider range of CLIP models with different scales of parameters and pre-train data. The results are summarized in Table 2 and further depicted in Figure 2(a). Generally speaking, performance drops can be observed across all considered CLIP configurations, indicating that CLIP models in various scales still learn spurious features. More specifically, we investigate the influence of a) parameter scales and b) pre-train data scales in CLIP models on the sensitivity of spurious features. We exclude the backbone of ViT-B/32 and the dataset of LAION400M to avoid biases in data collection.

Table 2: The 1 vs. 1000 results for CLIP checkpoints on the CounterAnimal dataset. The pre-train datasets with high-quality data are marked by *.

backbone	pre-train dataset	easy	hard	drop
RN-101	OpenAI	64.27	45.15	19.12
RN-50×4	OpenAI	70.02	49.07	20.95
ViT-B/16	LAION400M	73.11	52.17	20.94
ViT-B/16	OpenAI	73.08	56.56	16.52
ViT-B/16	DataComp1B*	80.36	64.24	16.12
ViT-B/16	LAION2B	73.18	53.18	20.00
ViT-B/16	DFN2B*	85.03	70.61	14.42
ViT-B/32	LAION400M	67.13	36.95	30.18
ViT-B/32	OpenAI	69.13	45.62	23.51
ViT-B/32	DataComp1B*	75.96	53.74	22.22
ViT-B/32	LAION2B	72.94	48.74	24.20
ViT-L/14	LAION400M	80.90	63.31	17.59
ViT-L/14	OpenAI	85.38	70.28	15.10
ViT-L/14	DataComp1B*	89.29	79.90	9.39
ViT-L/14	LAION2B	82.23	66.27	15.96
ViT-L/14	DFN2B*	90.77	80.55	10.22
ViT-L/14-336	OpenAI	86.36	73.14	13.21
ViT-H/14	LAION2B	85.74	73.13	12.61
ViT-H/14	DFN5B*	88.55	79.13	9.42
ViT-G/14	LAION2B	86.81	73.32	13.49
ViT-bigG/14	LAION2B	87.57	76.96	10.61

Scaling up Pre-train Data. To test the impacts of enlarging scales of pre-train datasets, we consider two CLIP backbones, namely, ViT-B/16 and ViT-L/14, along with a series of pre-train datasets of increasing sizes. The results are summarized in Figure 6. We observe that scaling up the data scale does not necessarily reduce the performance drop, suggesting that directly enlarging the scale of pre-train data alone cannot enhance robustness. One possible explanation is that larger datasets do not imply fewer biases, whereas the CLIP models will still inherit the spurious correlations therein.

Scaling up CLIP Model Sizes. We also explore the connection between model scales and spurious correlations. In Figure 7, we consider two pre-train datasets, namely, LAION2B and the close-soured

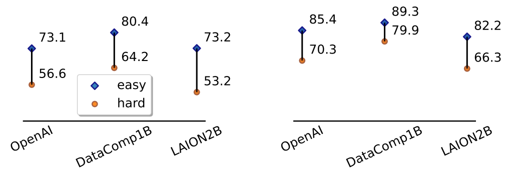

(a) ViT-B/16 (b) ViT-L/14

Figure 6: 1 vs. 1000 results for varying CLIP setups with different pre-train datasets.

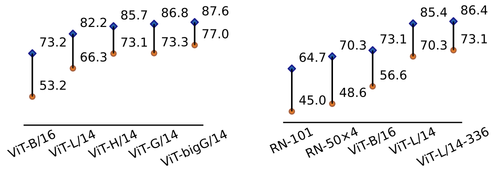

(a) LAION2B (b) OpenAI Checkpoints

Figure 7: 1 vs. 1000 results for varying CLIP setups with different backbones.

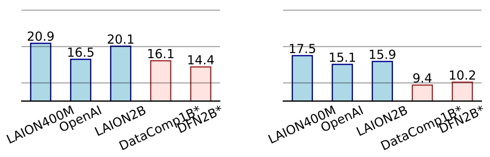

(a) ViT-B/16 (b) ViT-L/14

Figure 8: 1 vs. 1000 drops for varying CLIP setups with filtered and unfiltered pre-train data.

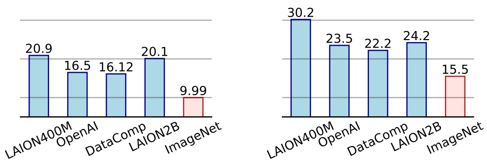

(a) ViT-B/16 (b) ViT-B/32

Figure 9: 1 vs. 1000 drops for varying training setups with CLIP and ImageNet supervision.

data from OpenAI, along with backbones of increasing scales. We observe a clear trend indicating that larger models exhibit better performance against spurious correlations. It may tell us that larger models possess stronger robustness, making them less prone to the shortcuts of spurious features.

Data Quality Matters. Moreover, we observe that the results obtained with DataComp- and DFN-trained CLIPs exhibit better performance and smaller drops across backbones, Figure 8 offers their comparisons. We notice that these datasets have been stringently filtered and thus possess high-quality data. It indicates that enhancing data quality is still a promising way to improve OOD generalization.

Our analysis focuses on absolute performance drop. In Appendix F, we strengthen our conclusions by incorporating the analysis based on effective robustness [5], where our findings still hold.

3.3 Evaluations for other Learning Paradigms

We extend our evaluations to broader families of models, including ImageNet-1K supervised models and more advanced LVLMs, such as MiniGPT4 and LLaVA.

ImageNet Models. We first extend our evaluations to include ImageNet models. The main results are summarized in Table 3. Moreover, Figure 9 further illustrates the accuracy drops of various CLIP models, in comparison to ImageNet models. Surprisingly, we find that ImageNet models are more robust to spurious features in CounterAnimal. This finding indicates that our CounterAnimal specifically characterizes the spurious features that are unique to CLIP configurations. Additionally, it indicates that spurious correlations in large-scale multi-modal data are distinct from that of the ImageNet scenarios which are widely used in conventional single-modal supervised learning. It further highlights the importance of our proposed dataset, which is especially suitable to study the spurious correlations for vision-language pre-training.

Table 3: The 1 vs. 1000 performance for ImageNet models CounterAnimal.

backbone	easy	hard	drop
AlexNet	59.56	39.24	20.31
VGG-11	73.37	56.12	17.25
VGG-13	75.33	58.43	16.90
VGG-19	77.84	61.74	16.10
RN-18	74.36	56.07	18.29
RN-34	78.31	61.01	17.30
RN-50	81.44	66.07	15.37
RN-101	81.76	68.18	13.57
ViT-B/16	84.97	74.98	9.99
ViT-B/32	79.84	64.36	15.48
ViT-L/16	83.74	72.69	11.05
ViT-L/32	81.23	67.54	13.69
ConvNext-S	88.27	79.97	8.30
ConvNext-B	88.60	80.53	8.07
ConvNext-L	89.12	81.47	7.65

Advanced LVLMs. We further evaluate for more advanced LVLMs, which align CLIP visual encoders with advanced large language models like Vi-

Table 4: The 1 vs. 20 results of `CounterAnimal` for advanced LVLMs and several CLIP models. More results of CLIP models and ImageNet models can be found in Appendix F.

LVLMs	`easy`	`hard`	drop
`MiniGPT4-Viccuna7B`	47.99	39.73	8.26
`LLaVA1.5-7B`	40.06	30.09	9.97
`CLIP-LAION400M-ViT-L/14`	80.90	63.31	17.59
`CLIP-OpenAI-ViT-L/14`	85.38	70.28	15.10
`CLIP-DataComp1B-ViT-L/14`	89.29	79.90	9.39
`CLIP-LAION2B-ViT-L/14`	82.23	66.27	15.96
`CLIP-DFN2B-ViT-L/14`	90.77	80.55	10.22

cuna [49]. To reduce inference costs, our evaluation follows the 1 vs. 20 setup. We summarize their results in Table 4, along with the 1 vs. 20 results for several CLIP models (cf., Appendix F for more results). We further depict the full results in Figure 2(b). As we can see, these advanced LVLMs have lower performance yet smaller drops, but the spurious features in `CounterAnimal` still impact them.

4 Understanding Why CLIPs Rely on Spurious Features

To better understand the observed phenomena in Section 3, we present a theoretical analysis of why the CLIP models rely on spurious features. We begin by establishing the setup for analyzing multi-modal contrastive learning following [9].

Definition 1 (Multi-modal Dataset)**.** *Consider n image-text pairs $\{(\boldsymbol{x}_I^i, \boldsymbol{x}_T^i)\}_{i=1}^n$, both image $\boldsymbol{x}_I^i$ and text $\boldsymbol{x}_T^i$ are generated from the latent factor $\boldsymbol{z}_i$, where $\boldsymbol{z} = [z_{inv}, z_{spu}] \in \mathbb{R}^2$ is composed of an invariant feature $z_{inv} \sim \mathcal{N}(\mu_{inv} y, \sigma_{inv}^2)$ and a spurious feature $z_{spu} \sim \mathcal{N}(\mu_{spu} a, \sigma_{spu}^2)$ with $\Pr(a = y) = p_{spu}$ otherwise $a = -y$. y is the label uniformly drawn from $\{-1, 1\}$. The training data $\mathcal{D}^{tr}$ is drawn with $\frac{1}{2} \leq p_{spu} \leq 1$ and OOD data $\mathcal{D}^*$ is drawn with a $p_{spu} = \frac{1}{2}$.*

We employ two linear encoders: $g_I : \mathbb{R}^{d_I} \to \mathbb{R}^h$ for the image modality and $g_T : \mathbb{R}^{d_T} \to \mathbb{R}^h$ for the text modality, implemented as $g_I(\boldsymbol{x}_I) = \boldsymbol{W}_I \boldsymbol{x}_I$ and $g_T(\boldsymbol{x}_T) = \boldsymbol{W}_T \boldsymbol{x}_T$ with $\boldsymbol{W}_I \in \mathbb{R}^{h \times d_I}$ and $\boldsymbol{W}_T \in \mathbb{R}^{h \times d_T}$. The encoders are trained through the linearized contrastive loss [9, 50] that mimics the CLIP dynamics:

$$\mathcal{L}_{\text{CLIP}} = \frac{1}{2n(n-1)} \sum_i \sum_{j \neq i} (s_{ij} - s_{ii}) + \frac{1}{2n(n-1)} \sum_i \sum_{j \neq i} (s_{ji} - s_{ii}) + \frac{\rho}{2} ||\boldsymbol{W}_I^T \boldsymbol{W}_T||_F^2, \tag{1}$$

where $s_{ij} = g_I(\boldsymbol{x}_I^i)^T g_T(\boldsymbol{x}_T^j)$ is the similarity with respect to the i-th image and j-th text representations. Once the CLIP (g_I, g_T) has been trained, the performance will be measured in a zero-shot manner by matching the most similar caption with the corresponding object name filled in, such as "`a photo of <object label>`" [2]. Intuitively, once the model focuses more on invariant features, it will have a better zero-shot classification accuracy across different distributions. Nevertheless, in the following theorem, we justify that CLIP remains to learn to use spurious features, aligning with our experimental observations on the `CounterAnimal` dataset.

Theorem 1. *Given a multi-modal dataset (Def. 1) with suitable variance in the features $\sigma_{inv} = \Theta(1) > \sigma_{spu}$, and spurious features with a large spurious correlation $p_{spu} = 1 - o(1)$, an overparameterized CLIP model where $n = \omega(1), d_M = \Omega(n)$ and $d_T = \Omega(n)$, if the spurious features (e.g., backgrounds of the image) takes up a relatively large amount of the image $\mu_{spu} \geq \frac{\sigma_{inv}^2 + 2}{2} \geq \mu_{inv} = 1$, then with a high probability of at least $1 - O(\frac{1}{poly(n)}) = 1 - o(1)$, the CLIP model achieves a large error in zero-shot accuracy in the OOD test data where $a \neq y$:*

$$Err(g_I, g_T) \geq 1 - \Phi(\kappa_1) - o(1),$$

and a small error in the OOD test data where $a = y$:

$$Acc(g_I, g_T) \geq 1 - \Phi(\kappa_2) - o(1),$$

where $\kappa_1 = \frac{\sigma_{inv}^2 + 2 - 2\mu_{spu} p_{spu}}{\sqrt{(1+\sigma_{inv}^2)^2 \sigma_{inv}^2 + (2\mu_{spu} p_{spu} - 1)^2 \sigma_{spu}^2}}$, $\kappa_2 = \frac{-2\mu_{spu} p_{spu} - \sigma_{inv}^2}{\sqrt{(1+\sigma_{inv}^2)^2 \sigma_{inv}^2 + (2\mu_{spu} p_{spu} - 1)^2 \sigma_{spu}^2}}$ and Φ denotes the CDF of a standard normal distribution.

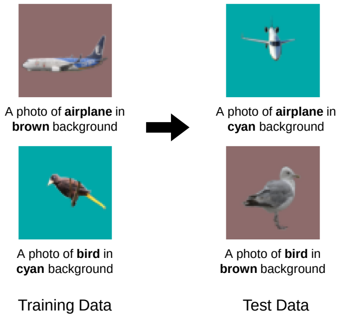
A photo of **airplane** in **brown** background
A photo of **airplane** in **cyan** background
A photo of **bird** in **cyan** background
A photo of **bird** in **brown** background
Training Data
Test Data

Figure 10: Illustration of ColoredCOCO.

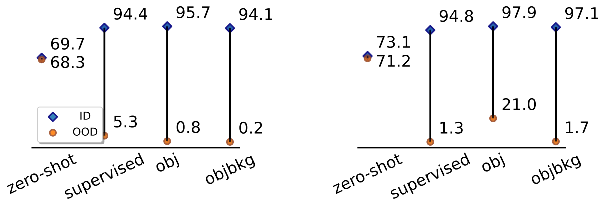

(a) OpenAI-RN-50 (b) OpenAI-ViT-B/16

Figure 11: CLIP performance on ColoredCOCO. "supervised" refers to supervised trained models, while "obj" and "objbkg" refer to using different prompts to fine-tune CLIPs.

We leave more theoretical details as well as the proof to Appendix D due to space limit. Intuitively, Theorem 1 implies that once there exists a relatively strong correlation between the object captions and the parts of image backgrounds, CLIP will learn to align the backgrounds, i.e., spurious features, with object captions. Although our theory discusses a simplistic case of one invariant and one spurious feature, there could exist more features describing the objects and even more features describing the backgrounds. CLIP will fail to robustly align the visual features of objects to its captions, once there exists a spurious correlation between any of the background features with the object caption. Our theory is the first to provably demonstrate the drawbacks of CLIPs in OOD generalization, providing the foundation for future developments tackling the issue.

To verify our theory, we construct multi-modal datasets named ColoredCOCO following [51]. It contains 9 classes and the spurious correlation in the training part is 80%, i.e., each class has a correlation of 80% to a specific biased color and 20% uniformly correlates to 10 different randomly chosen colors, cf., Figure 10. The OOD datasets are built with classes randomly correlating to other 8 biased colors. We consider two prompts with different descriptiveness: a) obj: "a photo of <object label>" and b) objbkg: "a photo of <object label> in <color label> background", with either objects or both objects and backgrounds.

We tune the pre-trained CLIP models using the CLIP objective, which has been shown to be most robust to distribution shifts [52]. In addition, we also incorporate the baseline of full fine-tuning with a new MLP onto the image encoder using the ERM objective. As shown in Figure 11, fine-tuning with CLIP objective based on neither of the prompts provides any non-trivial robustness against the vanilla full fine-tuning. The results further verify our theory. Nevertheless, the degraded robustness of CLIP could also be caused by the weak language understanding capability of the BERT encoder in the CLIP. To this end, we also conduct additional experiments with a perfect language encoder setting. The results are given in Appendix D.4. Nevertheless, we find that CLIP still performs similarly to ERM and is prone to distribution shifts even with perfect captions.

5 Conclusion

In this paper, we highlight biases in previous evaluations for assessing the robustness of CLIP models, primarily relying on ImageNet variants. Such improper benchmarking would cause illusions that CLIP models seem to resolve spurious correlations, particularly in comparison with ImageNet models. It motivates us to craft the new testset, named CounterAnimal, which is specifically designed to probe the natural spurious correlations between animal and their backgrounds. The spuriousness captured by CounterAnimal is general across different CLIP setups and exerts relatively small impacts on the ImageNet benchmarks, thereby specifically capturing the spurious correlations within CLIP setups. Our experiments on CounterAnimal show that many conventional strategies, e.g., increasing backbone scales and improving pre-train data quality, remain effective in enhancing the robustness of CLIP models. Moreover, we present a theoretical analysis for the reasons of the CLIP objective to learn biases. Overall, we provide a platform for future developments of more advanced and robust CLIP and vision-language models, and we hope our presented experiments can offer a sober look at the robustness of CLIP models to spurious correlations.

Acknowledgments

The authors would like to express their sincere gratitude to the anonymous reviewers and the area chairs for their thorough review and constructive feedback. Their insightful comments and valuable suggestions have significantly enhanced the quality and clarity of this manuscript. We deeply appreciate their time and effort in helping us improve our work.

References

[1] Jingyi Zhang, Jiaxing Huang, Sheng Jin, and Shijian Lu. Vision-language models for vision tasks: A survey. *IEEE Transactions on Pattern Analysis and Machine Intelligence*, 2024.

[2] Alec Radford, Jong Wook Kim, Chris Hallacy, Aditya Ramesh, Gabriel Goh, Sandhini Agarwal, Girish Sastry, Amanda Askell, Pamela Mishkin, Jack Clark, et al. Learning transferable visual models from natural language supervision. In *ICML*, 2021.

[3] Christoph Schuhmann, Romain Beaumont, Richard Vencu, Cade Gordon, Ross Wightman, Mehdi Cherti, Theo Coombes, Aarush Katta, Clayton Mullis, Mitchell Wortsman, et al. Laion-5b: An open large-scale dataset for training next generation image-text models. In *NeurIPS*, 2022.

[4] Samir Yitzhak Gadre, Gabriel Ilharco, Alex Fang, Jonathan Hayase, Georgios Smyrnis, Thao Nguyen, Ryan Marten, Mitchell Wortsman, Dhruba Ghosh, Jieyu Zhang, et al. Datacomp: In search of the next generation of multimodal datasets. *arXiv preprint arXiv:2304.14108*, 2023.

[5] Zhouxing Shi, Nicholas Carlini, Ananth Balashankar, Ludwig Schmidt, Cho-Jui Hsieh, Alex Beutel, and Yao Qin. Effective robustness against natural distribution shifts for models with different training data. In *NeurIPS*, 2023.

[6] Alex Fang, Gabriel Ilharco, Mitchell Wortsman, Yuhao Wan, Vaishaal Shankar, Achal Dave, and Ludwig Schmidt. Data determines distributional robustness in contrastive language image pre-training (CLIP). In *ICML*, 2022.

[7] Shibani Santurkar, Yann Dubois, Rohan Taori, Percy Liang, and Tatsunori Hashimoto. Is a caption worth a thousand images? a study on representation learning. In *ICLR*, 2023.

[8] Imant Daunhawer, Alice Bizeul, Emanuele Palumbo, Alexander Marx, and Julia E. Vogt. Identifiability results for multimodal contrastive learning. In *ICLR*, 2023.

[9] Yihao Xue, Siddharth Joshi, Dang Nguyen, and Baharan Mirzasoleiman. Understanding the robustness of multi-modal contrastive learning to distribution shift. *arXiv preprint arXiv:2310.04971*, 2023.

[10] Prasanna Mayilvahanan, Thaddäus Wiedemer, Evgenia Rusak, Matthias Bethge, and Wieland Brendel. Does CLIP's generalization performance mainly stem from high train-test similarity? In *NeurIPS 2023 Workshop on Distribution Shifts: New Frontiers with Foundation Models*, 2023.

[11] Mitchell Wortsman, Gabriel Ilharco, Jong Wook Kim, Mike Li, Simon Kornblith, Rebecca Roelofs, Raphael Gontijo Lopes, Hannaneh Hajishirzi, Ali Farhadi, Hongseok Namkoong, et al. Robust fine-tuning of zero-shot models. In *CVPR*, 2022.

[12] Martin Arjovsky, Léon Bottou, Ishaan Gulrajani, and David Lopez-Paz. Invariant risk minimization. *arXiv preprint arXiv:1907.02893*, 2019.

[13] Xiao Zhou, Yong Lin, Weizhong Zhang, and Tong Zhang. Sparse invariant risk minimization. In *International Conference on Machine Learning*, pages 27222–27244. PMLR, 2022.

[14] Yong Lin, Hanze Dong, Hao Wang, and Tong Zhang. Bayesian invariant risk minimization. In *Proceedings of the IEEE/CVF Conference on Computer Vision and Pattern Recognition*, pages 16021–16030, 2022.

[15] Xiao Zhou, Yong Lin, Renjie Pi, Weizhong Zhang, Renzhe Xu, Peng Cui, and Tong Zhang. Model agnostic sample reweighting for out-of-distribution learning. In *International Conference on Machine Learning*, pages 27203–27221. PMLR, 2022.

[16] Yong Lin, Fan Zhou, Lu Tan, Lintao Ma, Jiameng Liu, Yansu He, Yuan Yuan, Yu Liu, James Zhang, Yujiu Yang, et al. Continuous invariance learning. *arXiv preprint arXiv:2310.05348*, 2023.

https://doi.org/10.52202/079017-3893

[17] Yong Lin, Lu Tan, Yifan Hao, Honam Wong, Hanze Dong, Weizhong Zhang, Yujiu Yang, and Tong Zhang. Spurious feature diversification improves out-of-distribution generalization. *arXiv preprint arXiv:2309.17230*, 2023.

[18] Xiaoyu Tan, Lin Yong, Shengyu Zhu, Chao Qu, Xihe Qiu, Xu Yinghui, Peng Cui, and Yuan Qi. Provably invariant learning without domain information. In *International Conference on Machine Learning*, pages 33563–33580. PMLR, 2023.

[19] Yongqiang Chen, Kaiwen Zhou, Yatao Bian, Binghui Xie, Bingzhe Wu, Yonggang Zhang, MA KAILI, Han Yang, Peilin Zhao, Bo Han, and James Cheng. Pareto invariant risk minimization: Towards mitigating the optimization dilemma in out-of-distribution generalization. In *The Eleventh International Conference on Learning Representations*, 2023.

[20] Yongqiang Chen, Wei Huang, Kaiwen Zhou, Yatao Bian, Bo Han, and James Cheng. Understanding and improving feature learning for out-of-distribution generalization. In *Advances in Neural Information Processing Systems*, 2023.

[21] Andrei Barbu, David Mayo, Julian Alverio, William Luo, Christopher Wang, Dan Gutfreund, Josh Tenenbaum, and Boris Katz. Objectnet: A large-scale bias-controlled dataset for pushing the limits of object recognition models. *NeurIPS*, 2019.

[22] Joshua Vendrow, Saachi Jain, Logan Engstrom, and Aleksander Madry. Dataset interfaces: Diagnosing model failures using controllable counterfactual generation. *arXiv preprint arXiv:2302.07865*, 2023.

[23] Viraj Prabhu, Sriram Yenamandra, Prithvijit Chattopadhyay, and Judy Hoffman. Lance: Stress-testing visual models by generating language-guided counterfactual images. *NeurIPS*, 2023.

[24] Xiaodan Li, Yuefeng Chen, Yao Zhu, Shuhui Wang, Rong Zhang, and Hui Xue. Imagenet-e: Benchmarking neural network robustness via attribute editing. In *CVPR*, 2023.

[25] Jia Deng, Wei Dong, Richard Socher, Li-Jia Li, Kai Li, and Li Fei-Fei. Imagenet: A large-scale hierarchical image database. In *CVPR*, 2009.

[26] Dan Hendrycks, Kevin Zhao, Steven Basart, Jacob Steinhardt, and Dawn Song. Natural adversarial examples. In *CVPR*, 2021.

[27] Benjamin Recht, Rebecca Roelofs, Ludwig Schmidt, and Vaishaal Shankar. Do imagenet classifiers generalize to imagenet? In *ICML*, 2019.

[28] Alexey Dosovitskiy, Lucas Beyer, Alexander Kolesnikov, Dirk Weissenborn, Xiaohua Zhai, Thomas Unterthiner, Mostafa Dehghani, Matthias Minderer, Georg Heigold, Sylvain Gelly, et al. An image is worth 16x16 words: Transformers for image recognition at scale. *arXiv preprint arXiv:2010.11929*, 2020.

[29] Deyao Zhu, Jun Chen, Xiaoqian Shen, Xiang Li, and Mohamed Elhoseiny. Minigpt-4: Enhancing vision-language understanding with advanced large language models. *arXiv preprint arXiv:2304.10592*, 2023.

[30] Haotian Liu, Chunyuan Li, Qingyang Wu, and Yong Jae Lee. Visual instruction tuning. In *NeurIPS*, 2023.

[31] Alex Fang, Albin Madappally Jose, Amit Jain, Ludwig Schmidt, Alexander Toshev, and Vaishaal Shankar. Data filtering networks. *arXiv preprint arXiv:2309.17425*, 2023.

[32] Yu Yang, Besmira Nushi, Hamid Palangi, and Baharan Mirzasoleiman. Mitigating spurious correlations in multi-modal models during fine-tuning. *arXiv preprint arXiv:2304.03916*, 2023.

[33] Yifan Li, Yifan Du, Kun Zhou, Jinpeng Wang, Wayne Xin Zhao, and Ji-Rong Wen. Evaluating object hallucination in large vision-language models. *arXiv preprint*, arXiv:2305.10355, 2023.

[34] Shengbang Tong, Zhuang Liu, Yuexiang Zhai, Yi Ma, Yann LeCun, and Saining Xie. Eyes wide shut? exploring the visual shortcomings of multimodal llms. *arXiv preprint arXiv:2401.06209*, 2024.

[35] Qi Zhang, Yifei Wang, and Yisen Wang. On the generalization of multi-modal contrastive learning. In *ICML*, 2023.

[36] Haohan Wang, Songwei Ge, Zachary Lipton, and Eric P Xing. Learning robust global representations by penalizing local predictive power. *NeurIPS*, 2019.

[37] Kai Xiao, Logan Engstrom, Andrew Ilyas, and Aleksander Madry. Noise or signal: The role of image backgrounds in object recognition. *ArXiv preprint arXiv:2006.09994*, 2020.

[38] Rohan Taori, Achal Dave, Vaishaal Shankar, Nicholas Carlini, Benjamin Recht, and Ludwig Schmidt. Measuring robustness to natural distribution shifts in image classification. *NeurIPS*, 2020.

[39] Vaishaal Shankar, Achal Dave, Rebecca Roelofs, Deva Ramanan, Benjamin Recht, and Ludwig Schmidt. Do image classifiers generalize across time? In *ICCV*, 2021.

[40] Yong Lin, Shengyu Zhu, Lu Tan, and Peng Cui. Zin: When and how to learn invariance without environment partition? *NeurIPS*, 2022.

[41] Ishaan Gulrajani and David Lopez-Paz. In search of lost domain generalization. *arXiv preprint arXiv:2007.01434*, 2020.

[42] Shiori Sagawa, Pang Wei Koh, Tatsunori B Hashimoto, and Percy Liang. Distributionally robust neural networks for group shifts: On the importance of regularization for worst-case generalization. *arXiv preprint arXiv:1911.08731*, 2019.

[43] Gregory Plumb, Marco Tulio Ribeiro, and Ameet Talwalkar. Finding and Fixing Spurious Patterns with Explanations. *arXiv preprint arXiv:2106.02112*, 2021.

[44] X Li, Y Chen, Y Zhu, S Wang, R Zhang, and H ImageNet-E Xue. Benchmarking neural network robustness via attribute editing. In *CVPR*, 2023.

[45] Chenshuang Zhang, Fei Pan, Junmo Kim, In So Kweon, and Chengzhi Mao. Imagenet-d: Benchmarking neural network robustness on diffusion synthetic object. In *CVPR*, 2024.

[46] Yann Dubois, Yangjun Ruan, and Chris J Maddison. Optimal representations for covariate shifts. In *NeurIPS 2021 workshop on distribution shifts: connecting methods and applications*, 2021.

[47] Shiori Sagawa, Pang Wei Koh, Tatsunori B. Hashimoto, and Percy Liang. Distributionally robust neural networks. In *ICLR*, 2020.

[48] Mehdi Cherti, Romain Beaumont, Ross Wightman, Mitchell Wortsman, Gabriel Ilharco, Cade Gordon, Christoph Schuhmann, Ludwig Schmidt, and Jenia Jitsev. Reproducible scaling laws for contrastive language-image learning. In *CVPR*, 2023.

[49] Lianmin Zheng, Wei-Lin Chiang, Ying Sheng, Siyuan Zhuang, Zhanghao Wu, Yonghao Zhuang, Zi Lin, Zhuohan Li, Dacheng Li, Eric Xing, et al. Judging llm-as-a-judge with mt-bench and chatbot arena. *arXiv preprint arXiv:2306.05685*, 2023.

[50] Ryumei Nakada, Halil Ibrahim Gulluk, Zhun Deng, Wenlong Ji, James Zou, and Linjun Zhang. Understanding multimodal contrastive learning and incorporating unpaired data. In *AISTAT*, 2023.

[51] Faruk Ahmed, Yoshua Bengio, Harm van Seijen, and Aaron Courville. Systematic generalisation with group invariant predictions. In *ICLR*, 2021.

[52] Sachin Goyal, Ananya Kumar, Sankalp Garg, Zico Kolter, and Aditi Raghunathan. Finetune like you pretrain: Improved finetuning of zero-shot vision models. In *CVPR*, 2023.

[53] Jun Chen, Deyao Zhu, Xiaoqian Shen, Xiang Li, Zechun Liu, Pengchuan Zhang, Raghuraman Krishnamoorthi, Vikas Chandra, Yunyang Xiong, and Mohamed Elhoseiny. Minigpt-v2: large language model as a unified interface for vision-language multi-task learning. *arXiv preprint arXiv:2310.09478*, 2023.

[54] Shiori Sagawa, Aditi Raghunathan, Pang Wei Koh, and Percy Liang. An investigation of why overparameterization exacerbates spurious correlations. In *ICML*, 2020.

https://doi.org/10.52202/079017-3893

A Broader Impacts and Limitations

The current community often overestimates the robustness of CLIP models, largely due to the potentially misleading reliance on ImageNet variants for testing. To address this issue, we propose a new testset, named `CounterAnimal`, specifically tailored for CLIP models. Our findings indicate that CLIP models may not be as robust to distribution shifts as previously believed. Our dataset serves as a real-world benchmark, poised to be meaningful for the subsequent works to understand and enhance CLIP concerning their OOD robustness. For real-world applications, the understanding of spurious correlations for CLIP is also critical. We raise practical concerns when deploying CLIP models, which pertain to fairness and potential biases that may arise from inherent spurious correlations. We also present general strategies and theoretical analysis to understand the spurious correlations within CLIP models, which may motivate subsequent works to further enhance CLIP in real-world applications. However, although our dataset reaches the bar as a standard evaluation dataset, its research potential can be further benefited from expanding the scale of our dataset, diversifying the raw data sources beyond iNaturalist, broadening the semantic scope beyond animal classes, and studying other testbeds beyond the ImageNet benchmarks. In the future, we will extend our focus beyond animal subjects and include a wider array of high-quality data that are suitable for evaluating the robustness of CLIP and more advanced LVLMs.

B Dataset Composition

We release our dataset `CounterAnimal` structured as follows:

```
CounterAnimal
├── ostrich
│   ├── easy-ground
│   │   ├── figure1.jpeg
│   │   ├── figure2.jpg
│   │   └── ...
│   └── hard-water
│       ├── figure1.jpeg
│       ├── figure2.jpg
│       └── ...
├── brambling
│   ├── easy-green
│   │   ├── figure1.jpeg
│   │   ├── figure2.jpg
│   │   └── ...
│   └── hard-sky
│       ├── figure1.jpeg
│       ├── figure2.jpg
│       └── ...
└── ...
```

Overall, the `CounterAnimal` dataset is organized by the object names. The data therein are further separated into two parts, i.e., the `easy` and `hard` groups, where the background name is also provided for each sub-directory. By evaluating accuracy with respect to the `easy` and `hard` groups, one can quantify the impacts of the spurious correlations captured by `CounterAnimal`. We further summarize the ImageNet animal objects as well as the group names for the `easy` and `hard` groups in Table 5.

C Experimental Configurations

In this section, we provide more details about our experimental configurations.

C.1 Hardware Configurations

All experiments are realized by Pytorch 1.81 with CUDA 11.1, using machines equipped with GeForce RTX 3090 GPUs and AMD Threadripper 3960X Processors.

Table 5: The object names and the background names in the `CounterAnimal` dataset. The full names of labels are presented following the fashion of the ImageNet-1K dataset.

ID	object label	easy	hard	ID	object label	easy	hard	ID	object label	easy	hard
1	ostrich, struthio camelus	ground	water	2	brambling, Fringilla montifringilla	grass	sky	3	bulbul	sky	grass
4	water ouzel, dipper	water	ground	5	vulture	sky	tree	6	bullfrog, rana catesbeiana	water	ground
7	loggerhead, loggerhead turtle, caretta caretta	water	ground	8	box turtle, box tortoise	grass	earth	9	common iguana,iguana iguana iguana	earth	shrub
10	whiptail, whiptail lizard	earth	human	11	agama	rock	tree	12	african crocodile, nile crocodile, crocodylus niloticus	earth	grass
13	hognose snake, puff adder, sand viper	earth	grass	14	king snake kingsnake	earth	grass	15	garter snake grass snake	grass	earth
16	water snake	water	ground	17	harvestman, daddy longlegs, Phalangium opilio	shrub	rock	18	scorpion	indoor	outdoor
19	tarantula	sand	grass	20	centipede	indoor	grass	21	black grouse	grass	tree
22	ptarmigan	snow	grass	23	prairie chicken, prairie grouse, prairie fowl	grass	snow	24	sulphur-crested cockatoo, Kakatoe galerita, cacatua galerita	tree	grass
25	black swan, cygnus atratus	water	ground	26	echidna, spiny anteater, anteater	grass	tree	27	black stork ciconia nigra	grass	sky
28	flamingo	water	sky	29	bittern	grass	tree	30	pelican	water	sky
31	sea lion	sand	water	32	african hunting dog, hyena dog, cape hunting dog, lycaon pictus	grass	tree	33	hyena, hyaena	grass	road
34	red fox, vulpes vulpes	grass	road	35	arctic fox, white fox, alopex lagopus	snow	grass	36	jaguar, panther, Panthera onca, Felis onca	water	tree
37	lion, king of beasts, panthera leo	grass	tree	38	cheetah, chetah, acinonyx jubatus	grass	tree	39	ice bear, polar bear, ursus maritimus, thalarctos maritimus	snow	grass
40	dung beetle	earth	human	41	cicada, cicala	tree	human	42	beaver	water	grass
43	bighorn, bighorn sheep, cimarron	grass	rock	44	mink	grass	water	45	otter	water	tree

C.2 Candidate Label Space

We consider two different label spaces of candidate labels: a) using the full ImageNet-1K class names and b) using the top-20 most confusing classes for more computing-intensive models like MiniGPT4. It leads to the following two evaluation setups, i.e., the 1 vs. 1000 setup and the 1 vs. 20 setup.

1 vs. 1000 Setup. As a default option, we use the full label space of the ImageNet-1K dataset, which is suitable given that the object labels for `CounterAnimal` all belong to that of the ImageNet-1K dataset. Furthermore, this choice also reflects a more realistic situation in the open world, where we have a vast number of candidate labels and the failure cases of LVLMs are common.

1 vs. 20 Setup. To suit more advanced LVLMs of which the inference costs are much higher than CLIP models, we constrain the sizes of candidate label space for each class. Specifically, based on `CLIP-LAION400M-ViT-B/32`, we select the top-20 most confusing labels, which is calculated by the average cosine similarity for both the `easy` and `hard` groups.

C.3 Evaluation Metrics

Now, we discuss the evaluation metrics. Typically, they are applied to the `easy` and `hard` groups separately when we evaluate the robustness of various models.

Class-wise Accuracy. We are interested in the effects of spurious features for each class. Therefore, we calculate the prediction accuracy specifically for photos within each class. It can be referred to as the class-wise accuracy, which is given by

$$\texttt{ACC}(\texttt{label}) = \frac{1}{|\mathcal{I}_{\texttt{label}}|} \sum_{i \in \mathcal{I}_{\texttt{label}}} \mathbf{1}\{\hat{y}_i = \texttt{label}\},$$

where $\mathcal{I}_{\texttt{label}}$ is the indices of photos belonging to `label` and $\hat{y}_i$ is the predicted label for the i-th image. The class-wise accuracy reflects the class-level model reliability against spurious correlations.

Average Accuracy. Upon the class-wise accuracy, we can calculate the average performance of models, namely,

$$\texttt{ACC} = \frac{1}{|\mathcal{L}|} \sum_{\texttt{label} \in \mathcal{L}} \texttt{ACC}(\texttt{label}).$$

Compared to the conventional average accuracy, i.e., $\frac{1}{|\mathcal{I}|} \sum_{i \in \mathcal{I}} \mathbf{1}\{\hat{y}_i = \texttt{gt}\}$ with $\mathcal{I}$ the image indices and `gt` the true labels, our definition of the average accuracy further offsets the impact of class

Table 6: Adopted versions of CLIP checkpoints employed in our main experiments.

backbone	pre-train dataset	checkpoint
ViT-B/16	LAION400M	E31
ViT-B/16	LAION2B	S34B B88K
ViT-B/16	DataComp1B	XL S13B B90K
ViT-B/32	LAION400M	E31
ViT-B/32	LAION2B	S34B B79K
ViT-B/32	DataComp1B	XL S13B B90K
ViT-L/14	LAION400M	E31
ViT-L/14	LAION2B	S32B B82K
ViT-L/14	DataComp1B	XL S32B B82K
ViT-H/14	LAION2B	S32B B79K
ViT-G/14	LAION2B	S34B B88K
ViT-bigG/14	LAION2B	S34B B160K
ConvNext-B	LAION400M	S13B B51K
ConvNext-BW	LAION2B	S13B B82K

imbalance. We default to using the average accuracy, and present the results without balancing in Tables 17-18 for CLIP and ImageNet models.

Accuracy Drop. To quantify the spurious correlations that make CLIP models fail, we measure the performance drop when moving from the `easy` and `hard` groups. At the class level, the accuracy drop is defined as the class-wise accuracy of `easy` minuses that of `hard`. At the dataset level, it is the average value for the class-level accuracy drop.

C.4 Evaluation Details of MiniGPT4 and LLaVA

To evaluate LVLMs with a backend of language models, we follow the common practice that constructs questions to prompt LVLMs [29, 30]. Specifically, we construct the question as:

```
What is the main object in the image?
```

and then calculate the language modeling loss with respect to the answer:

```
A <object name>
```

for each ImageNet class name. Meanwhile, we also try another question prompt that is widely used in training MiniGPT4 and LLaVA [30, 53]:

```
Describe this image in detail.
```

while the performance will generically decrease. In addition, when we switch to the object-centric evaluation protocol as [33]:

```
Is there a <object name> in the image?
```

or

```
Is this image a photo of <object name>?
```

and evaluate the answer with `Yes` for each class, we observe a severe performance decrease as LVLMs easily hallucinate the objects. If we strictly follow the evaluation metrics of [33] by simply fetching the answers instead of comparing the losses, there exist lots of hallucinated objects by LVLMs in our dataset.

C.5 CLIP Naming Rules

For the CLIP checkpoints, we adopt the naming rule of "`CLIP-<dataset>-<backbone>`", where `<dataset>` is the name of pre-train datasets and `<backbone>` is the specific name of backbone models. For example, `CLIP-LAION400M-ViT-B/32` indicates the `ViT-B/32` model CLIP-trained on `LAION400M`. Different training setups are considered in OpenCLIP, and the versions of the adopted checkpoints are summarized in Table 6. Moreover, in Table 15, we consider the results of checkpoints beyond the adopted ones.

D Theoretical Understanding of CLIP's Robustness to Spurious Features

We provide a more detailed setup and analysis in complementary to Section 4.

D.1 Detailed Theoretical Setup

We begin by introducing more details about the data generation process following the literature [9, 50, 54].

Definition 2 (Multi-modal Dataset). *Consider n image-text pairs $\{(\boldsymbol{x}_I^i, \boldsymbol{x}_T^i)\}_{i=1}^n$, both image $\boldsymbol{x}_I^i \in \mathbb{R}^{d_I}$ and text $\boldsymbol{x}_T^i \in \mathbb{R}^{d_T}$ are generated from the underlying latent factor $\boldsymbol{z}_i \in \mathbb{R}^l$. The samples are generated as follows:*

- *$\boldsymbol{z} = [z_{inv}, z_{spu}] \in \mathbb{R}^2$ is composed of a invariant feature $z_{inv} \sim \mathcal{N}(\mu_{inv} y, \sigma_{inv}^2)$ and a spurious feature $z_{spu} \sim \mathcal{N}(\mu_{spu} a, \sigma_{spu}^2)$ with $\Pr(a = y) = p_{spu}$ otherwise $a = -y$, y is the label uniformly drawn from $\{-1, 1\}$, $\mathcal{D}^{tr}$ is drawn with $1/2 \leq p_{spu} \leq 1$ while the OOD test data $\mathcal{D}^*$ is drawn uniformly with $p_{spu} = 1/2$.*
- *Given $\boldsymbol{z}$, the $\boldsymbol{x}$ at modality M is generated via $\boldsymbol{x}_M = \boldsymbol{D}_M \boldsymbol{\mu}_M(\boldsymbol{z}) + \xi_M$, with $\boldsymbol{D}_M \in \mathbb{R}^{d_M \times l}$ and $\xi_M \sim \mathcal{N}(0, \sigma_\xi^2 / d_m \boldsymbol{I}_{d_m})$. The matrix $\boldsymbol{D}_M \in \mathbb{R}^{d_m \times l}$ with $d_m > l$ is a matrix with orthonormal columns which can be considered as a dictionary matrix.*

With the definition, we can write every $\boldsymbol{z}^i = \begin{bmatrix} y^i + \eta_{1,i} \\ \mu_{spu} p_{spu} + \eta_{2,i} \end{bmatrix}$ where $\eta_{1,i}, \eta_{2,i}$ are two Gaussian variables in the definition.

CLIP Training. We employ two linear encoders $g_I : \mathbb{R}^{d_I} \to \mathbb{R}^h$ for the image modality and $g_T : \mathbb{R}^{d_T} \to \mathbb{R}^h$ for the text modality, implemented as $g^I(\boldsymbol{x}_I) = \boldsymbol{W}_I \boldsymbol{x}_I$ and $g_T(\boldsymbol{x}_T) = \boldsymbol{W}_T \boldsymbol{x}_T$ with $\boldsymbol{W}_I \in \mathbb{R}^{h \times d_I}$ and $\boldsymbol{W}_T \in \mathbb{R}^{h \times d_T}$, respectively. The encoders are trained through the linearized contrastive loss [9, 50] that mimics CLIP training dynamics:

$$
\begin{aligned}
\mathcal{L}_{\text{CLIP}} = & \frac{1}{2n(n-1)} \sum_i \sum_{j \neq i} (s_{ij} - s_{ii}) \\
& + \frac{1}{2n(n-1)} \sum_i \sum_{j \neq i} (s_{ji} - s_{ii}) + \frac{\rho}{2} ||\boldsymbol{W}_I^T \boldsymbol{W}_T||_F^2,
\end{aligned}
\tag{2}
$$

where $s_{ij} = g_I(\boldsymbol{x}_I^i)^T g_T(\boldsymbol{x}_T^j)$ is the similarity with respect to the i-th image and j-th text representations, and $||\boldsymbol{W}_I^T \boldsymbol{W}_T||_F^2$ is the a regularization term with $\rho > 0$.

Zero-shot Inference. Once the CLIP model (g_I, g_T) is trained, the performance will be measured in a zero-shot manner by matching the most similar caption such as `'a photo of {object name}'` across different `object name` as class names. Meanwhile, one could also leverage several prompts and leverage the average text embeddings across the available prompts to facilitate the evaluation [2]. The prompt with respect to y could be modeled as $\boldsymbol{p}_y = \boldsymbol{D}_T \mathbb{E}[\boldsymbol{z}^t | y]$, where $\boldsymbol{D}_T$ is the prompt transformation matrix. Then, the zero-shot accuracy of CLIP could be formalized as follows:

$$
\text{Acc}(g_I, g_T) = \mathbb{E}_{(\boldsymbol{x}, y)}[\mathbf{1}(\arg\max_{\hat{y}} g_I(\boldsymbol{x}_I)^T g_T(\boldsymbol{p}_{\hat{y}}), y)],
\tag{3}
$$

while the error is $\text{Err}(g_I, g_T) = 1 - \text{Acc}(g_I, g_T)$. Intuitively, once the model extracts more of the invariant features, it will have a better zero-shot classification accuracy across different distributions.

D.2 Proof for Theorem 1

Theorem 2 (Restatement of Theorem 1). *Given a multi-modal dataset (Def. 2) with suitable variance in the features $\sigma_{inv} = \Theta(1) > \sigma_{spu}$, and spurious features with a large spurious correlation $p_{spu} = 1 - o(1)$, an overparameterized CLIP model where $n = \omega(1), d_M = \Omega(n)$ and $d_T = \Omega(n)$, if the spurious features (e.g., backgrounds of the image) takes up a relatively large amount of the image $\mu_{spu} \geq \frac{\sigma_{inv}^2 + 2}{2} \geq \mu_{inv} = 1$, then with a high probability of at least $1 - O(\frac{1}{poly(n)}) = 1 - o(1)$, the CLIP model achieves a large error in zero-shot accuracy in the OOD test data where $a \neq y$:*

$$
Err(g_I, g_T) \geq 1 - \Phi(\kappa_1) - o(1),
$$

and a small error in the OOD test data where $a = y$:

$$Acc(g_I, g_T) \geq 1 - \Phi(\kappa_2) - o(1),$$

where $\kappa_1 = \frac{\sigma_{inv}^2 + 2 - 2\mu_{spu}p_{spu}}{\sqrt{(1+\sigma_{inv}^2)^2\sigma_{inv}^2 + (2\mu_{spu}p_{spu}-1)^2\sigma_{spu}^2}}$, $\kappa_2 = \frac{-2\mu_{spu}p_{spu} - \sigma_{inv}^2}{\sqrt{(1+\sigma_{inv}^2)^2\sigma_{inv}^2 + (2\mu_{spu}p_{spu}-1)^2\sigma_{spu}^2}}$ *and* Φ *denotes the CDF of a standard normal distribution.*

Proof. We will introduce some useful lemmas to help with our proof.

Lemma 1 ([9])**.** *The minimizer of linearized CLIP loss* $\boldsymbol{W}_I^{*T}\boldsymbol{W}_T^*$ *satisfies the following with a probability of at least* $1 - O(\frac{1}{poly(n)})$ *such that,*

$$||\boldsymbol{W}_I^{*T}\boldsymbol{W}_T^* - \frac{1}{\rho}\boldsymbol{D}_I \begin{bmatrix} 1+\sigma_{inv}^2 & 2\mu_{spu}p_{spu}-1 \\ 2\mu_{spu}p_{spu}-1 & 1+\sigma_{spu}^2 \end{bmatrix} \boldsymbol{D}_T^T||_2 \leq \frac{1}{\rho}O(\sqrt{\epsilon_0}),$$

where $\epsilon_0 = O(\sqrt{\frac{\log n}{n}})$.

Intuitively, the lemma indicates the importance of the training distribution, that the minimizer of CLIP will converge to the data characteristics of the latent features of the training distribution.

Then, consider the case where the model is inferred onto a test sample with $y = 1, a = -1$. Then, with the aforementioned lemma, we have

$$\begin{aligned} |\boldsymbol{x}_I^T\boldsymbol{W}_I^*\boldsymbol{W}_T^*\boldsymbol{x}_T^{\hat{y}} - \frac{1}{\rho}\boldsymbol{x}_I^T\boldsymbol{D}_I \begin{bmatrix} 1+\sigma_{inv}^2 & 2\mu_{spu}p_{spu}-1 \\ 2\mu_{spu}p_{spu}-1 & 1+\sigma_{spu}^2 \end{bmatrix} \boldsymbol{D}_T^T\boldsymbol{x}_T^{\hat{y}}||_2 &\leq ||\boldsymbol{x}_I|| ||\boldsymbol{x}_T^{\hat{y}}|| \frac{1}{\rho}O(\sqrt{\epsilon_0}) \\ &\leq \frac{1}{\rho}O(\sqrt{\epsilon_0}\log n). \end{aligned} \tag{4}$$

Then, notice that

$$\frac{1}{\rho}\boldsymbol{x}_I^T\boldsymbol{D}_I \begin{bmatrix} 1+\sigma_{inv}^2 & 2\mu_{spu}p_{spu}-1 \\ 2\mu_{spu}p_{spu}-1 & 1+\sigma_{spu}^2 \end{bmatrix} \boldsymbol{D}_T^T\boldsymbol{x}_T^{\hat{y}} = \hat{y}((1+\eta_1)(1+\sigma_{inv}^2)+(-1+\eta_2)(2\mu_{spu}p_{spu}-1). \tag{5}$$

When CLIP makes an incorrect prediction, we have

$$\boldsymbol{x}_I^T\boldsymbol{W}_I^*\boldsymbol{W}_T^*\boldsymbol{x}_T^{\hat{y}=1} < \boldsymbol{x}_I^T\boldsymbol{W}_I^*\boldsymbol{W}_T^*\boldsymbol{x}_T^{\hat{y}=-1}.$$

Then, we have

$$\begin{aligned} &\frac{1}{\rho}\boldsymbol{x}_I^T\boldsymbol{D}_I \begin{bmatrix} 1+\sigma_{inv}^2 & 2\mu_{spu}p_{spu}-1 \\ 2\mu_{spu}p_{spu}-1 & 1+\sigma_{spu}^2 \end{bmatrix} \boldsymbol{D}_T^T\boldsymbol{x}_T^{\hat{y}=1} - \frac{1}{\rho}O(\sqrt{\epsilon_0}\log n) < \\ &\frac{1}{\rho}\boldsymbol{x}_I^T\boldsymbol{D}_I \begin{bmatrix} 1+\sigma_{inv}^2 & 2\mu_{spu}p_{spu}-1 \\ 2\mu_{spu}p_{spu}-1 & 1+\sigma_{spu}^2 \end{bmatrix} \boldsymbol{D}_T^T\boldsymbol{x}_T^{\hat{y}=-1} - \frac{1}{\rho}O(\sqrt{\epsilon_0}\log n), \end{aligned} \tag{6}$$

with Eq. 5 plugged in, denote $\epsilon_1 = O(\sqrt{\epsilon_0}\log n)$, we further have

$$-2\left[(1+\eta_1)(1+\sigma_{inv}^2) + (-1+\eta_2)(2\mu_{spu}p_{spu}-1) - \epsilon_1\right] > 0. \tag{7}$$

Since $\eta_1(1+\sigma_{inv}^2) + \eta_2(2\mu_{spu}p_{spu}-1)$ is a Gaussian variable follows the distribution of

$$\eta_1(1+\sigma_{inv}^2) + \eta_2(2\mu_{spu}p_{spu}-1) \sim \mathcal{N}(0, (1+\sigma_{inv}^2)^2\sigma_{inv}^2 + (2\mu_{spu}p_{spu}-1)^2\sigma_{spu}^2),$$

then, we have

$$\begin{aligned} &\Pr(-2\left[(1+\eta_1)(1+\sigma_{inv}^2) + (-1+\eta_2)(2\mu_{spu}p_{spu}-1) - \epsilon_1\right] > 0) \\ &= \Pr_{v\sim\mathcal{N}(0,1)}(v > \frac{\sigma_{inv}^2 + 2 - 2\mu_{spu}p_{spu} + \epsilon_1}{\sqrt{(1+\sigma_{inv}^2)^2\sigma_{inv}^2 + (2\mu_{spu}p_{spu}-1)^2\sigma_{spu}^2}}) \\ &= 1 - \Phi(\frac{\sigma_{inv}^2 + 2 - 2\mu_{spu}p_{spu} + \epsilon_1}{\sqrt{(1+\sigma_{inv}^2)^2\sigma_{inv}^2 + (2\mu_{spu}p_{spu}-1)^2\sigma_{spu}^2}}), \end{aligned} \tag{8}$$

Table 7: Comparison between CLIPs and standard supervised learning on ColoredCOO

backbone	pre-train dataset	approach	in-distribution	out-of-distribution	drop
RN-50	OpenAI	zero shot	69.67	68.33	1.34
RN-50	OpenAI	obj	95.67	0.78	94.89
RN-50	OpenAI	objbkg	94.11	0.22	93.89
RN-50	OpenAI	supervised	94.44	5.33	89.11
ViT-B/16	OpenAI	zero shot	73.11	71.22	1.89
ViT-B/16	OpenAI	obj	97.89	21	76.89
ViT-B/16	OpenAI	objbkg	97.11	1.67	95.44
ViT-B/16	OpenAI	supervised	94.78	1.33	93.45

where Φ is the CDF of the standard Gaussian distribution. Then, it suffices to know that the $\text{Err}_{y=1,a=-1}$ is lower bounded by $\Phi(\frac{\sigma_{inv}^2+2-2\mu_{spu}p_{spu}+\epsilon_1}{\sqrt{(1+\sigma_{inv}^2)^2\sigma_{inv}^2+(2\mu_{spu}p_{spu}-1)^2\sigma_{spu}^2}})$, which also applies to the case $y=-1, a=1$.

Similarly, given the case $y=a$, as the model fits the spurious feature, we could derive the lower bound for its Acc by leveraging the spurious features as $\Phi(\frac{-2\mu_{spu}p_{spu}-\sigma_{inv}^2}{\sqrt{(1+\sigma_{inv}^2)^2\sigma_{inv}^2+(2\mu_{spu}p_{spu}-1)^2\sigma_{spu}^2}})$. $\square$

D.3 More Details on ColoredCOO Experiments

To further validate our theoretical results, we construct the ColoredCOO dataset following [51]. More specifically, ColoredCOO is constructed as follows:

- The dataset contains 9 classes of COCO objects. The spurious correlation in the trainset is 80% such that each class has a correlation of 80% to a specific biased color and 20% uniformly correlates to 10 sufficiently different randomly chosen colors.
- The OOD testsets are constructed with classes randomly correlating to 8 biased colors different from the one correlated in the training set.

Then, we further generate two prompts for each sample:

1. `obj`: `a photo of <object label>`;
2. `objbkg`: `a photo of <object label> in <color label> background`

We tune the pre-trained CLIP models using the CLIP objective based on the OpenCLIP library. We consider the learning rate of $\{1e-3, 1e-4, 1e-5\}$, with a weight decay of $\{1e-1, 1e-3, 1e-5\}$, and a warmup of $\{0, 1000\}$ steps. We select the model according to the best in-distribution test performance. The detailed results are given in Table 7. As we can see, the CLIPs finetuned using either the CLIP objective or the standard supervised training both exhibit high sensitivity to the spurious features.

D.4 More Details on MultiColoredMNIST Experiments

One possible explanation for the failure of CLIP objective in ColoredCOCO is that, the language encoder of the CLIP models may not understand the captions well. Therefore, we further construct a new setup called MultiColoredMNIST, where each image contains only the digit information from MNIST dataset and the color information. Therefore, we can directly derive the one hot encoding for all of the useful factors in the dataset.

Data. We consider a multi-class classification setting with a number of classes no less than 2. The objects are the

- Training data: Fix two class (0/1) and color (r/g), they are spurious correlated by a correlation p_{spu}. The invariant feature's correlation with labels is p_{inv}.
- Test data (Rand): All classes and the colors are randomly correlated, given k class, $p_{spu} = 1/k$.
- Test data (Rev): All classes and the colors are reversely correlated, p_{spu} is 10% 0/1 classes and $1/k$ for others.

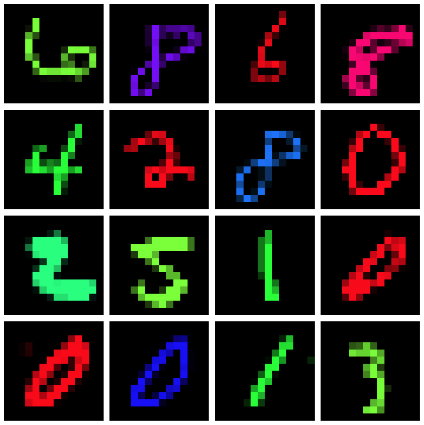

Figure 12: Examples of `MultiColoredMNIST` dataset.

In Figure 12, we give some examples for the `MultiColoredMnist` dataset.

Experimental setting. We compare the standard supervised training and CLIP. To avoid noises or information loss in encoding language modality, we consider the perfect language supervision for a single model. Given a batch of image and caption representations $\{(\boldsymbol{h}^{x_i}, \boldsymbol{h}^{c_i})\}_i^B$, for a image-caption pair, the CLIP objective aims to

$$\max(\boldsymbol{M}_x\boldsymbol{h}^{x_i} \cdot \boldsymbol{M}_c\boldsymbol{h}^{c_i}) - (\boldsymbol{M}_x\boldsymbol{h}^{x_j} \cdot \boldsymbol{M}_c\boldsymbol{h}^{c_j}), \forall i \neq j, \tag{9}$$

where $\boldsymbol{M}_x \in \mathbb{R}^{d\times h_x}$ and $\boldsymbol{M}_c^{d\times h_c}$ are the learnable projection layers for image and caption representations. Assuming the perfect language encoding as the one-hot encoding for all possible object and background appearance $\boldsymbol{h}^{c_i} \in [0,1]^{|\mathcal{O}|+|\mathcal{B}|}$, and $\boldsymbol{M}_c$ can simply be an identity matrix, then Eq. 9 can be considered as a classification task for objects and backgrounds respectively:

$$\max \mathrm{CE}(\boldsymbol{M}_c^T\boldsymbol{M}_x\boldsymbol{h}^{x_i}, \boldsymbol{h}^{c_i}), \tag{10}$$

where the labels are simply the one-hot encodings of the objects and the backgrounds, and the classifier is $\boldsymbol{M}_c^T\boldsymbol{M}_x$. For the `MultiColoredMNIST` task where there is only one object and background (i.e., color), to implement Eq. 10, we only need to construct an additional classification head for the background. Given the aforementioned setup, we conduct experiments comparing CLIP-based contrastive learning to the standard supervised learning. The results are given in Table 8. As we can see, both contrastive learning and supervised learning perform similarly across different numbers of classes and bias degrees.

https://doi.org/10.52202/079017-3893

Table 8: Comparison of standard supervised learning and contrastive learning on `MultiColoredMNIST` dataset.

# classes	# samples	p_{inv}	p_{spu}	train method	class 0/1 (Rand)	class 0/1 (Rev.)	rest class
2	10,610	0.9	0.75	Contrastive	87.42±0.79	81.87±1.86	n/a
2	10,610	0.9	0.75	Supervised	86.44±0.90	80.22±1.73	n/a
2	10,610	0.9	0.9	Contrastive	71.56±1.79	50.08±3.97	n/a
2	10,610	0.9	0.9	Supervised	71.62±1.58	50.13±3.24	n/a
2	10,610	0.75	0.75	Contrastive	65.06±2.21	43.18±3.78	n/a
2	10,610	0.75	0.75	Supervised	65.01±1.68	43.76±3.44	n/a
2	10,610	0.75	0.9	Contrastive	53.73±1.08	16.42±1.74	n/a
2	10,610	0.75	0.9	Supervised	53.89±0.96	17.14±1.88	n/a
3	15,578	0.9	0.75	Contrastive	85.86±0.70	81.88±0.52	88.33±1.48
3	15,578	0.9	0.75	Supervised	85.03±1.25	79.20±1.91	88.03±1.10
3	15,578	0.9	0.9	Contrastive	69.05±2.26	45.55±4.52	88.60±1.20
3	15,578	0.9	0.9	Supervised	68.29±1.37	44.74±3.50	88.43±0.89
3	15,578	0.75	0.75	Contrastive	61.57±2.86	37.76±2.81	68.84±3.53
3	15,578	0.75	0.75	Supervised	59.51±2.28	36.66±2.06	68.75±2.58
3	15,578	0.75	0.9	Contrastive	42.47±2.48	7.08±1.10	71.07±3.01
3	15,578	0.75	0.9	Supervised	41.60±1.67	8.18±0.95	71.89±1.55
5	25,538	0.9	0.75	Contrastive	86.06±0.56	82.41±0.77	88.30±0.39
5	25,538	0.9	0.75	Supervised	85.60±0.74	80.99±0.99	87.76±0.57
5	25,538	0.9	0.9	Contrastive	71.78±0.77	44.66±4.02	88.15±0.42
5	25,538	0.9	0.9	Supervised	70.73±1.41	43.47±4.01	87.80±0.59
5	25,538	0.75	0.75	Contrastive	61.15±1.10	33.97±3.70	71.88±0.79
5	25,538	0.75	0.75	Supervised	57.69±1.29	33.66±3.18	68.75±0.91
5	25,538	0.75	0.9	Contrastive	35.37±1.70	4.60±0.45	72.47±0.58
5	25,538	0.75	0.9	Supervised	34.82±1.97	5.44±0.70	69.38±0.59
6	30,044	0.9	0.75	Contrastive	85.76±0.74	81.87±1.41	86.58±0.54
6	30,044	0.9	0.75	Supervised	85.84±0.81	81.81±1.27	86.29±0.47
6	30,044	0.9	0.9	Contrastive	70.99±2.39	40.07±10.53	86.57±0.49
6	30,044	0.9	0.9	Supervised	70.97±2.45	40.63±9.81	86.25±0.52
6	30,044	0.75	0.75	Contrastive	62.05±1.18	32.70±4.50	70.76±0.40
6	30,044	0.75	0.75	Supervised	59.49±1.26	33.94±3.69	67.91±0.81
6	30,044	0.75	0.9	Contrastive	38.96±2.55	4.71±0.56	70.65±0.40
6	30,044	0.75	0.9	Supervised	35.85±2.27	4.87±0.71	68.36±0.91
8	40,170	0.9	0.75	Contrastive	84.81±0.86	80.54±1.27	86.43±0.40
8	40,170	0.9	0.75	Supervised	85.49±0.67	81.47±1.08	86.78±0.39
8	40,170	0.9	0.9	Contrastive	71.75±1.65	39.85±8.81	86.34±0.36
8	40,170	0.9	0.9	Supervised	72.82±1.37	41.36±7.19	86.78±0.39
8	40,170	0.75	0.75	Contrastive	63.73±1.96	31.46±7.20	71.08±0.57
8	40,170	0.75	0.75	Supervised	62.22±2.00	33.12±6.54	70.58±0.63
8	40,170	0.75	0.9	Contrastive	43.91±2.36	5.11±0.68	70.76±0.60
8	40,170	0.75	0.9	Supervised	40.39±2.82	5.28±0.92	70.43±0.64
10	50,000	0.9	0.75	Contrastive	84.52±0.77	80.42±1.70	85.19±0.27
10	50,000	0.9	0.75	Supervised	85.10±0.67	81.83±0.97	86.11±0.15
10	50,000	0.9	0.9	Contrastive	73.79±1.43	48.02±5.50	85.18±0.34
10	50,000	0.9	0.9	Supervised	74.97±1.69	52.09±5.72	85.96±0.24
10	50,000	0.75	0.75	Contrastive	65.31±1.43	32.31±6.73	69.67±0.53
10	50,000	0.75	0.75	Supervised	66.00±1.52	36.35±5.59	70.27±0.30
10	50,000	0.75	0.9	Contrastive	48.03±1.56	5.53±1.25	69.13±0.47
10	50,000	0.75	0.9	Supervised	46.83±1.33	5.72±1.35	69.92±0.37

E Ablation Studies

In this section, we present ablation studies to further validate the feasibility of our data curation process.

Biasing to ImageNet Setups. We follow the same curation procedure while using ImageNet models (i.e., ResNet50-ImageNet) to construct `easy` and `hard` splits, where we name the corresponding dataset as `CounterAnimal-I`. We present the results of CLIP and ImageNet models on `CounterAnimal-I` in Tables 9-10, respectively. The effective robustness is further shown in Figure 13. Contrary to the observations within original `CounterAnimal`, CLIP models can demonstrate better robustness against spurious features within `CounterAnimal-I`. It aligns with our expectation since different training data (e.g., LAION for CLIPs, and ImageNet for ImageNet models) follow different distributions and naturally contain different spurious features. It also demonstrates the generality of our data curation method to reveal the spurious features for different kinds of the models. We also list the background names for `easy` and `hard` splits with respect to some of the selected classes in Table 11. As observed, using different models to split data will capture very different spurious features. It highlights the necessity to curate an OOD testset for CLIP models, as CLIP models learn different spurious features than ImageNet models.

Correctness vs. Frequency. We further explain why `easy` and `hard` examples can characterize spurious features within CLIP setups. In general, spurious features can be caused by biases inherent in the data distribution concerning backgrounds. For example, for the animal class of `ice bear`, the background of `ice` is more common than other backgrounds, such as `grass`, thus causing spurious correlations learned by CLIP models. Therefore, we investigate in terms of the background frequency, employing the searching tool of `Have I Been Trained` [4] that can retrieve images from LAION5B closely matching a given class name. We examine 10 animal classes as our case studies. For each class, we collect the top 100 most relevant images and tally the occurrences of the backgrounds of our consideration. It is important to note that our counting process excludes cartoon images, irrelevant photos, corrupted photos, and those featuring multiple distinct animal subjects or ambiguous backgrounds. The results are summarized in Table 12. As we can see, in general, the spurious features captured align with our conjecture that hard examples contain uncommon backgrounds in the CLIP training data, e.g., LAION5B, further justifying the feasibility of our `CounterAnimal` in assessing the robustness of CLIP models in real-world situations.

[4] `https://haveibeentrained.com`

Table 9: The 1 vs. 1000 results for CLIP checkpoints on the CounterAnimal-I dataset.

backbone	pre-train dataset	easy	hard	drop
RN-50	OpenAI	60.90	42.56	18.34
RN-101	OpenAI	61.22	40.25	20.97
RN-50×4	OpenAI	64.40	47.85	16.55
RN-50×16	OpenAI	72.00	57.65	14.35
RN-50×64	OpenAI	81.41	68.36	13.05
ViT-B/16	LAION400M	73.71	53.22	20.49
ViT-B/16	OpenAI	73.46	56.56	17.10
ViT-B/16	DataComp1B*	79.33	63.10	16.23
ViT-B/16	LAION2B	68.66	52.13	16.53
ViT-B/16	DFN2B*	83.39	68.75	14.64
ViT-B/32	LAION400M	57.32	37.61	19.71
ViT-B/32	OpenAI	66.95	47.12	19.84
ViT-B/32	DataComp1B*	73.59	53.99	19.60
ViT-B/32	LAION2B	67.37	47.64	19.73
ViT-B/32-256	DataComp1B*	78.18	60.80	17.39
ViT-L/14	LAION400M	77.96	60.85	17.11
ViT-L/14	OpenAI	81.67	67.55	14.12
ViT-L/14	DataComp1B*	88.87	77.06	11.82
ViT-L/14	LAION2B	78.89	63.14	15.75
ViT-L/14	DFN2B*	88.72	77.51	11.21
ViT-L/14-336	OpenAI	84.09	71.62	12.47
ViT-H/14	LAION2B	83.77	71.04	12.72
ViT-H/14	DFN5B*	89.32	79.65	9.68
ViT-H/14-384	DFN5B*	92.55	83.19	9.36
ViT-G/14	LAION2B	84.46	68.16	16.31
ViT-bigG/14	LAION2B	86.39	74.03	12.36
ConvNext-B	LAION400M	52.06	38.85	14.22
ConvNext-BW	LAION2B	57.19	38.74	18.45

Table 10: The 1 vs. 1000 performance for ImageNet models on the CounterAnimal-I dataset.

backbone	easy	hard	drop
AlexNet	59.27	31.87	27.40
VGG-11	73.82	46.66	27.15
VGG-13	74.32	48.08	26.24
VGG-19	77.07	52.77	24.30
RN-18	73.08	49.19	23.89
RN-34	77.52	52.74	24.78
RN-50	80.71	52.97	27.74
RN-101	82.35	59.46	22.90
ViT-B/16	85.06	66.64	18.42
ViT-B/32	78.27	55.42	22.85
ViT-L/16	83.65	64.03	19.63
ViT-L/32	80.28	59.17	21.11
ConvNext-S	88.87	73.86	15.01
ConvNext-B	88.92	74.48	14.44
ConvNext-L	89.88	77.21	12.67

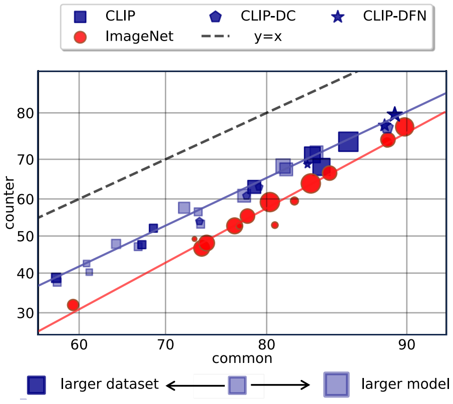

Figure 13: The easy verus hard performance (%) for CLIP and ImageNet models on CounterAnimal-I. The 1 vs. 1000 setup is considered.

Table 11: Selected animal object and background names in CounterAnimal and CounterAnimal-I. We bold the background names differently between CounterAnimal and CounterAnimal-I.

object label	CounterAnimal		CounterAnimal-I	
	easy	hard	easy	hard
Ostrich	ground	**water**	ground	**rock**
Brambling	grass	**sky**	grass	**water**
Bulbul	sky	**tree**	sky	**grass**
Vluture	sky	tree	sky	tree
Box turtle	grass	**earth**	grass	**water**
Common iguana	earth	shrub	earth	shrub
Whiptail	**earth**	**human**	**water**	**shurb**
Agama	rock	**tree**	rock	**grass**
Crocodile	earth	**grass**	earth	**tree**

Table 12: The number of photos counted with respect to easy and hard backgrounds, based on the searching tool of Have I Been Trained.

object label	easy		hard	
	name	number	name	number
ostrich	ground	30	water	0
brambling	grass	9	sky	17
bulbul	sky	5	grass	3
water ouzel	water	31	ground	4
bullfrog	water	28	ground	19
vulture	grass	9	sky	1
box turtle	grass	5	earth	3
loggerhead	water	8	grass	0
whiptail	earth	58	human	2
agama	rock	50	tree	8
african crocodile	earth	15	grass	8
hognose snake	earth	34	grass	14
king snake	earth	24	grass	21
garter snake	grass	36	earth	28
water snake	water	34	ground	29
harvestman	shrub	40	rock	27
scorpion	indoor	2	outdoor	4
tarantula	sand	41	grass	6
centipede	indoor	1	grass	4
black grouse	grass	41	tree	3
ptarmigan	snow	13	grass	15
prairie chicken	grass	61	snow	1
sulphur-crested cockatoo	tree	51	grass	14
black swan	water	13	ground	0
echidna	grass	9	tree	0
black stork	grass	35	sky	20
flamingo	water	1	sky	0
bittern	grass	28	tree	9
pelican	water	19	sky	4
sea lion	sand	22	water	19
african hunting dog	grass	78	tree	3
hyena	grass	36	road	8
red fox	grass	24	road	4
arctic fox	snow	23	grass	26
jaguar	water	0	tree	3
lion	grass	4	tree	2
cheetah	grass	26	tree	2
ice bear	snow	17	grass	1
dung beetle	earth	52	human	0
cicada	tree	13	human	0
beaver	water	6	grass	7
bighorn	grass	20	rock	3
mink	grass	1	water	1
otter	water	14	tree	3

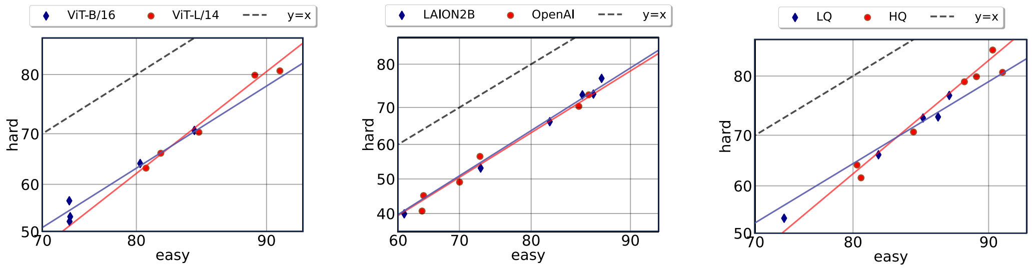

(a) Backbones (b) Datasets (c) Data Quality

Figure 14: Comparison for the effective robustness with respect to a) different backbones, b) different pre-train datasets, as well as c) high-quality (HQ) and low-quality (LQ) pre-train datasets.

F More Results

In this section, we present more experimental results to support our claims.

Effective Robustness. In Section 3, we mainly examine the absolute robustness to assess and compare the OOD performance across various CLIP setups, which are well known to be sensitive to the original value scales. Therefore, in Figure 14, we apply the measures of effective robustness [5] to further substantiate our conclusions. Overall, our previous conclusions are upheld, demonstrating that the benefits derived from increasing model scales and enhancing data quality notably outweigh those obtained by merely expanding dataset sizes.

Top-5 Results for CLIP models. We present 1 vs. 1000 results for more CLIP checkpoints on the `CounterAnimal` dataset in Table 13, which is an extension of Table 2. Moreover, we present more results for the evaluations on `CounterAnimal`, supplementing our analysis of CLIP models under spurious correlations. To begin with, we report the top-5 scores under the 1 vs. 1000 setup, where we check if the target label is one of the top-5 model predictions. The results are summarized in Table 14. Comparing with the top-1 results in Table 13, we find that there is still a large performance gap between the `easy` and `hard` groups, indicating that the label confusion is quite diverse and not limited to the top two classes.

Other Versions of Pre-train Datasets. OpenCLIP provides other CLIP checkpoints beyond our adopted ones. Table 15 summarizes the results of CLIP models similar to Table 2 while using different versions of checkpoints. As we can see, the performance for both `easy` and `hard` is very stable across varying versions, except for `DataComp1B`. The reason is that their various checkpoints use subsets of `DataComp1B`, where `XL` indicates the fully `DataComp1B`, `L` indicates a 140M subset, `M` indicates a 14M subset, and `S` indicates a 1.4M subset.

Results of OpenAI Prompts. We further consider the prompt setups following OpenAI CLIP [2], using average text embeddings over 80 predefined prompts as the final text embeddings. The results are summarized in Table 16. As we can see, the average performance for both the `easy` and `hard` groups generally improves 1 to 3 percentage points over the results of our simpler prompt. However, our main conclusion remains unchanged: the ImageNet models generally exhibit better performance and smaller drops. Another interesting finding is that when evaluating with `CLIP-LAION400M-ViT-B/32` (the CLIP checkpoint employed in our data collection), the performance drop with OpenAI prompts is not as high as that of our simple prompt used in Table 2. It indicates that our curation procedure mainly overfit the adopted prompt instead of the particular CLIP checkpoint.

Average Performance without Balancing. We by default adopt the balanced average accuracy to offset the impacts of class imbalance. In Tables 17-18, we further summarize the results without class balance, following $\frac{1}{|\mathcal{I}|}\sum_{i\in\mathcal{I}}\mathbf{1}\{\hat{y}_i=\mathtt{gt}\}$. As we can see, the performance drop remains obvious, and similar conclusions can be drawn as the balanced results: a) Backbone scales are more important for spurious robustness than pre-train dataset scales, and b) ImageNet models are more reliable when facing spurious features in `CounterAnimal`.

1 vs. 20 Results for CLIP and ImageNet Models. We adopt the 1 vs. 20 setup for the evaluations of more advanced LVLMs in Table 4. For a fair comparison, we further summarize the 1 vs. 20

Table 13: The 1 vs. 1000 results for CLIP checkpoints on CounterAnimal. The pre-train datasets with high-quality data are marked by *.

backbone	pre-train dataset	easy	hard	drop
RN-50	OpenAI	64.02	40.70	23.32
RN-101	OpenAI	64.27	45.15	19.12
RN-50×4	OpenAI	70.02	49.07	20.95
RN-50×16	OpenAI	76.43	59.13	17.30
RN-50×64	OpenAI	80.25	66.77	13.48
ViT-B/16	LAION400M	73.11	52.17	20.94
ViT-B/16	OpenAI	73.08	56.56	16.52
ViT-B/16	DataComp1B*	80.36	64.24	16.12
ViT-B/16	LAION2B	73.18	53.18	20.00
ViT-B/16	DFN2B*	85.03	70.61	14.42
ViT-B/32	LAION400M	67.13	36.95	30.18
ViT-B/32	OpenAI	69.13	45.62	23.51
ViT-B/32	DataComp1B*	75.96	53.74	22.22
ViT-B/32	LAION2B	72.94	48.74	24.20
ViT-B/32-256	DataComp1B*	80.72	61.65	19.07
ViT-L/14	LAION400M	80.90	63.31	17.59
ViT-L/14	OpenAI	85.38	70.28	15.10
ViT-L/14	DataComp1B*	89.29	79.90	9.39
ViT-L/14	LAION2B	82.23	66.27	15.96
ViT-L/14	DFN2B*	90.77	80.55	10.22
ViT-L/14-336	OpenAI	86.36	73.14	13.21
ViT-H/14	LAION2B	85.74	73.13	12.61
ViT-H/14	DFN5B*	88.55	79.13	9.42
ViT-H/14-384	DFN5B*	90.23	83.67	6.56
ViT-G/14	LAION2B	86.81	73.32	13.49
ViT-bigG/14	LAION2B	87.57	76.96	10.61
ConvNext-B	LAION400M	59.85	36.77	23.08
ConvNext-BW	LAION2B	61.03	39.91	21.12

results for CLIP models in Table 19 and for ImageNet models in Table 20. As we can see, there does not exist a significant change in performance drop compared to 1 vs. 1000 results, indicating that mistakes made by CLIP models are relatively concentrated. As in Figure 2, we also depict the easy versus hard performance for various learning setups with their names, following the 1 vs. 1000 setup in Figure 15 and 1 vs. 20 setups in Figure 16.

Class-wise Results. In Tables 21-22, we summarize the detailed results of the class-wise accuracy for the main results in Figure 5. We further depict the drop in accuracy in Figure 17. Generally speaking, the spurious features found in CLIP-LAION400M-ViT-B/32 can also fail other CLIP setups, and the general trends of decline are preserved class-wise. However, there are some cases where the drop in accuracy between easy and hard is negative, e.g., for data in class ID 33 and 42. It means that for these cases, our collection pipeline may have a large overfit to the adopted CLIP setup, i.e., CLIP-LAION400M-ViT-B/32.

Table 14: The 1 vs. 1000 results with top-5 performance scores for CLIP checkpoints on CounterAnimal. The pre-train datasets with high-quality data are marked by *.

backbone	pre-train dataset	easy	hard	drop
RN-50	OpenAI	91.02	77.15	13.87
RN-101	OpenAI	89.04	79.98	9.06
RN-50×4	OpenAI	91.21	83.65	7.55
RN-50×16	OpenAI	92.72	87.65	7.55
RN-50×64	OpenAI	95.22	92.35	2.87
ViT-B/16	LAION400M	92.54	84.03	8.51
ViT-B/16	OpenAI	94.74	88.21	6.53
ViT-B/16	DataComp1B*	95.04	90.89	4.15
ViT-B/16	LAION2B	91.04	84.64	6.40
ViT-B/16	DFN2B*	95.45	91.98	3.48
ViT-B/32	LAION400M	87.54	71.48	16.06
ViT-B/32	OpenAI	91.28	81.29	9.99
ViT-B/32	DataComp1B*	92.60	85.88	6.72
ViT-B/32	LAION2B	90.73	81.47	9.25
ViT-B/32-256	DataComp1B*	94.26	88.33	5.93
ViT-L/14	LAION400M	94.33	88.73	5.60
ViT-L/14	OpenAI	96.12	93.19	2.93
ViT-L/14	DataComp1B*	97.36	95.10	2.26
ViT-L/14	LAION2B	93.24	89.76	3.48
ViT-L/14	DFN2B*	96.76	94.53	2.23
ViT-L/14-336	OpenAI	96.60	94.30	2.30
ViT-H/14	LAION2B	95.26	91.72	3.55
ViT-H/14	DFN5B*	97.03	94.51	2.52
ViT-H/14-384	DFN5B*	97.02	95.45	1.57
ViT-G/14	LAION2B	95.30	91.20	4.10
ViT-bigG/14	LAION2B	95.31	93.01	2.29
ConvNext-B	LAION400M	81.67	69.90	11.77
ConvNext-BW	LAION2B	82.64	73.27	9.37

Table 15: The 1 vs. 1000 performance with other versions of CLIP checkpoints in OpenCLIP.

backbone	pre-train dataset	checkpoint	easy	hard	drop
ViT-B/16	LAION400M	E31	73.11	52.17	20.94
ViT-B/16	LAION400M	E32	73.59	52.53	21.06
ViT-B/16	DataComp1B	XL S13B B90K	80.36	64.24	16.12
ViT-B/16	DataComp1B	L S1B B8K	65.80	44.14	21.66
ViT-B/32	LAION400M	E31	67.13	36.95	30.18
ViT-B/32	LAION400M	E32	67.13	36.98	30.15
ViT-B/32	LAION2B	E16	71.32	47.21	24.11
ViT-B/32	LAION2B	S34B B79K	72.94	48.74	24.20
ViT-B/32	DataComp1B	XL S13B B90K	75.96	53.74	22.22
ViT-B/32	DataComp1B	M S128M B4K	25.91	11.65	14.26
ViT-B/32	DataComp	S S13M B4K	0.02	0.01	0.01
ViT-L/14	LAION400M	E31	80.90	63.31	17.59
ViT-L/14	LAION400M	E32	81.11	63.87	17.24
ViT-G/14	LAION2B	S12B B42K	83.72	68.46	15.26
ViT-G/14	LAION2B	S34B B88K	86.81	73.32	13.49

Table 16: The 1 vs. 1000 performance using prompts of OpenAI CLIP. The pre-train datasets with high-quality data are marked by *.

backbone	pre-train dataset	easy	hard	drop
RN-50	OpenAI	64.55	44.20	20.35
RN-101	OpenAI	64.81	46.30	18.51
RN-50×4	OpenAI	69.62	53.68	15.93
RN-50×16	OpenAI	84.78	72.13	12.65
RN-50×64	OpenAI	84.33	72.02	12.31
ViT-B/16	LAION400M	76.20	58.17	18.18
ViT-B/16	OpenAI	76.58	60.58	16.00
ViT-B/16	DataComp1B*	82.85	69.74	13.11
ViT-B/16	LAION2B	74.08	58.18	15.90
ViT-B/16	DFN2B*	85.20	74.33	10.87
ViT-B/32	LAION400M	66.68	43.22	23.46
ViT-B/32	OpenAI	67.23	47.11	20.12
ViT-B/32	DataComp1B*	76.00	59.23	16.77
ViT-B/32	LAION2B	70.25	50.00	20.25
ViT-B/32-256	DataComp1B*	79.77	64.20	15.57
ViT-L/14	LAION400M	81.22	65.31	15.91
ViT-L/14	OpenAI	85.76	73.23	12.53
ViT-L/14	DataComp1B*	89.56	81.21	8.35
ViT-L/14	LAION2B	83.43	69.44	13.99
ViT-L/14	DFN2B*	90.45	82.28	8.17
ViT-L/14-336	OpenAI	86.45	76.30	10.15
ViT-H/14	LAION2B	86.11	75.30	10.81
ViT-H/14	DFN5B*	91.33	85.20	6.13
ViT-H/14-384	DFN5B*	92.20	88.01	4.19
ViT-G/14	LAION2B	87.17	77.20	10.97
ViT-bigG/14	LAION2B	87.57	76.96	10.61
ConvNext-B	LAION400M	60.20	44.15	16.05
ConvNext-BW	LAION2B	63.33	46.11	17.22

Table 17: The 1 vs. 1000 performance on CounterAnimal for CLIP models, evaluating based on the accuracy without balancing. The pre-train datasets with high-quality data are marked by *.

backbone	pre-train dataset	easy	hard	drop
RN-50	OpenAI	64.59	38.40	26.19
RN-101	OpenAI	64.18	43.99	20.19
RN50-×4	OpenAI	70.76	46.91	23.85
RN50-×16	OpenAI	77.26	58.97	18.29
RN50-×64	OpenAI	82.88	62.84	20.04
ViT-B/16	LAION400M	75.58	48.46	27.12
ViT-B/16	OpenAI	73.94	53.93	20.01
ViT-B/16	DataComp1B*	81.83	61.47	20.36
ViT-B/16	LAION2B	74.97	51.20	23.77
ViT-B/16	DFN2B*	86.10	67.95	18.14
ViT-B/32	LAION400M	69.02	33.94	35.08
ViT-B/32	OpenAI	68.84	44.17	24.67
ViT-B/32	DataComp1B*	78.16	51.50	26.66
ViT-B/32	LAION2B	74.23	46.36	27.87
ViT-B/32-256	DataComp1B*	82.38	58.56	23.82
ViT-L/14	LAION400M	81.06	61.68	19.38
ViT-L/14	OpenAI	85.29	69.25	16.04
ViT-L/14	DataComp1B*	90.79	77.28	13.51
ViT-L/14	LAION2B	83.47	62.33	21.14
ViT-L/14	DFN2B*	91.81	78.10	13.71
ViT-L/14-336	OpenAI	86.40	72.40	14.00
ViT-H/14	LAION2B	87.10	69.84	17.26
ViT-H/14	DFN5B*	90.36	76.19	14.17
ViT-H/14-384	DFN5B*	92.29	80.95	11.34
ViT-G/14	LAION2B	88.09	69.96	18.13
ViT-bigG/14	LAION2B	88.47	73.45	15.02
ConvNext-B	LAION400M	60.16	34.27	25.89
ConvNext-BW	LAION2B	60.65	38.64	22.01

Table 18: The 1 vs. 1000 performance on CounterAnimal for ImageNet models, evaluating based on the accuracy without balancing.

backbone	easy	hard	drop
AlexNet	62.33	37.20	25.12
VGG-11	75.92	53.35	22.57
VGG-13	77.23	55.58	21.65
VGG-19	79.40	58.93	20.47
RN-18	76.46	52.79	23.67
RN-34	80.38	57.80	22.58
RN-50	83.52	62.97	20.54
RN-101	83.58	64.74	18.84
ViT-B/16	86.97	71.62	15.35
ViT-B/32	82.03	61.71	20.32
ViT-L/16	85.96	70.21	15.75
ViT-L/32	82.89	64.64	18.25
ConvNext-S	89.88	76.61	13.27
ConvNext-B	90.27	77.51	12.76
ConvNext-L	90.67	78.34	12.33

Table 19: The 1 versus 20 performance on CounterAnimal for CLIP models. The pre-train datasets with high-quality data are marked by *.

backbone	pre-train dataset	easy	hard	drop
RN-50	OpenAI	67.41	43.63	23.78
RN-101	OpenAI	66.92	47.23	19.69
RN-50×4	OpenAI	71.82	50.50	21.32
RN-50×16	OpenAI	78.60	60.63	17.97
RN-50×64	OpenAI	82.33	69.05	13.28
ViT-B/16	LAION400M	75.51	54.59	20.92
ViT-B/16	OpenAI	75.89	58.74	17.15
ViT-B/16	DataComp1B*	82.02	66.02	16.00
ViT-B/16	LAION2B	75.85	55.48	20.37
ViT-B/16	DFN2B*	86.04	72.13	13.91
ViT-B/32	LAION400M	70.46	39.44	31.02
ViT-B/32	OpenAI	72.17	49.25	22.92
ViT-B/32	DataComp1B*	78.58	56.32	22.26
ViT-B/32	LAION2B	75.68	51.86	23.82
ViT-B/32-256	DataComp1B*	83.05	63.98	19.07
ViT-L/14	LAION400M	82.27	64.89	17.38
ViT-L/14	OpenAI	86.38	72.12	14.26
ViT-L/14	DataComp1B*	90.13	80.46	9.67
ViT-L/14	LAION2B	83.81	67.68	16.13
ViT-L/14	DFN2B*	91.29	81.23	10.05
ViT-L/14-336	OpenAI	87.56	75.16	12.40
ViT-H/14	LAION2B	86.75	74.29	12.46
ViT-H/14	DFN5B*	89.13	79.79	9.35
ViT-H/14-384	DFN5B*	90.70	84.00	6.70
ViT-G/14	LAION2B	87.74	74.11	13.63
ViT-bigG/14	LAION2B	88.35	77.85	10.50
ConvNext-B	LAION400M	64.85	39.71	25.14
ConvNext-BW	LAION2B	65.61	44.21	21.40

Table 20: The 1 versus 20 performance on CounterAnimal for ImageNet models.

backbone	easy	hard	drop
AlexNet	67.71	46.43	21.29
VGG-11	77.25	60.19	17.06
VGG-13	79.07	62.02	17.04
VGG-19	80.80	65.19	15.61
RN-18	78.11	59.47	18.64
RN-34	81.14	64.32	16.82
RN-50	83.72	68.60	15.29
RN-101	84.13	70.77	13.37
ViT-B/16	86.57	76.88	9.69
ViT-B/32	82.56	68.30	14.26
ViT-L/16	85.71	74.94	10.77
ViT-L/32	83.86	71.00	12.86
ConvNext-S	89.31	81.61	7.69
ConvNext-B	89.58	82.32	7.26
ConvNext-L	89.84	82.67	7.17

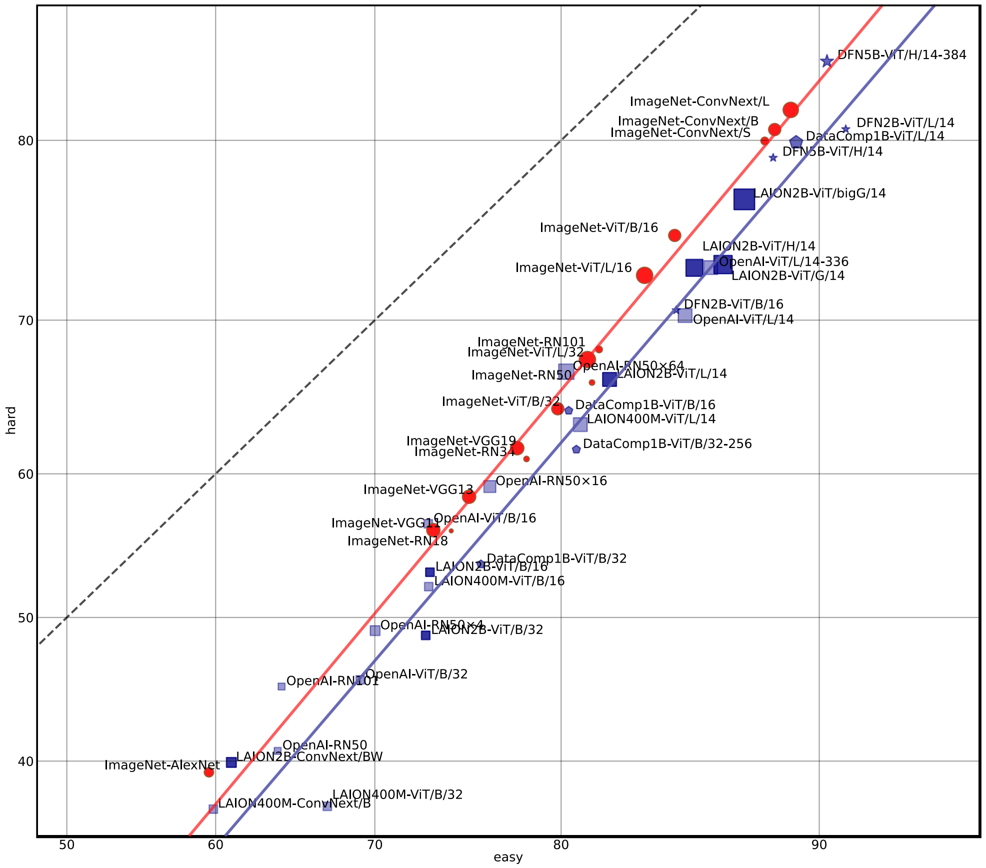

Figure 15: The `easy` versus `hard` performance (%) for CLIP and ImageNet models, following the 1 vs. 1000 setup. We also present the model setups for each `easy`-`hard` result pair.

https://doi.org/10.52202/079017-3893

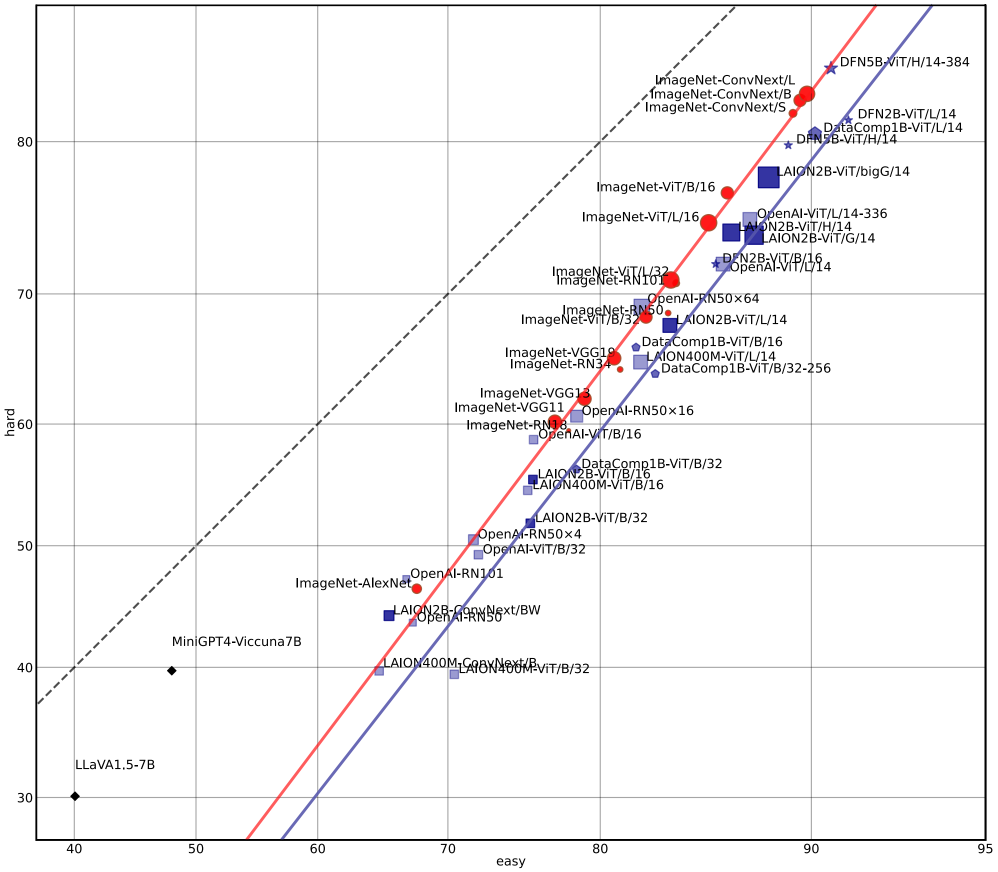

Figure 16: The `easy` versus `hard` performance (%) for CLIP, ImageNet models, and more advanced LVLMs, following the 1 vs. 20 setup. We also present the model setups for each `easy-hard` result pair.

Table 21: Class-wise 1 vs. 1000 performance on CounterAnimal for different backbones CLIP-trained on LAION400M.

class ID	CLIP-LAION400M-ViT-B/16			CLIP-LAION400M-ViT-B/32			CLIP-LAION400M-ViT-L/14		
	easy	hard	drop	easy	hard	drop	easy	hard	drop
1	71.36	64.60	6.76	79.61	57.52	22.09	93.20	91.15	2.05
2	87.18	69.37	17.81	78.63	49.55	29.08	94.02	75.68	18.34
3	18.85	8.65	10.20	28.69	14.59	14.09	14.75	7.57	7.19
4	90.00	70.99	19.01	81.15	48.15	33.01	94.23	90.12	4.11
5	76.19	67.35	8.84	87.76	41.84	45.92	97.96	82.65	15.31
6	88.32	67.72	20.60	73.36	48.10	25.26	83.94	68.35	15.59
7	78.64	43.96	34.68	73.64	18.68	54.96	81.36	69.23	12.13
8	69.23	44.00	25.23	73.85	49.00	24.85	87.69	74.00	13.69
9	74.00	37.50	36.50	54.00	30.83	23.17	54.00	39.17	14.83
10	79.92	26.00	53.92	60.64	4.00	56.64	69.48	13.00	56.48
11	62.43	28.87	33.55	74.26	28.87	45.39	60.95	42.96	17.99
12	83.52	51.19	32.33	72.53	35.71	36.81	89.01	72.62	16.39
13	64.04	26.83	37.21	22.17	2.44	19.73	17.24	7.32	9.92
14	63.60	53.06	10.54	32.46	22.45	10.01	64.04	44.90	19.14
15	61.54	22.09	39.45	67.95	19.68	48.27	85.90	18.47	67.42
16	82.12	13.50	68.62	68.87	1.23	67.65	88.08	50.92	37.16
17	56.09	52.00	4.09	48.50	20.00	28.50	77.25	52.80	24.45
18	68.35	54.92	13.43	29.11	4.17	24.95	87.34	69.32	18.02
19	83.98	74.05	9.93	81.82	43.67	38.15	91.34	70.89	20.46
20	67.21	59.62	7.60	55.74	20.19	35.55	75.41	70.19	5.22
21	67.31	37.12	30.19	73.08	43.94	29.14	71.15	56.82	14.34
22	87.72	57.01	30.71	96.49	67.29	29.20	100.00	80.37	19.63
23	85.33	50.57	34.75	59.85	17.24	42.60	83.78	41.38	42.40
24	98.77	78.00	20.77	88.34	63.00	25.34	98.77	95.00	3.77
25	98.04	88.68	9.36	93.63	68.87	24.76	99.02	86.79	12.23
26	5.60	1.81	3.79	20.00	4.07	15.93	43.20	8.60	34.60
27	86.42	62.42	24.00	77.78	14.77	63.01	85.19	78.52	6.66
28	65.48	27.72	37.76	79.70	55.45	24.25	91.37	82.18	9.19
29	92.20	67.92	24.27	80.49	39.62	40.87	95.12	83.02	12.10
30	96.98	82.83	14.15	86.21	71.72	14.49	99.14	93.94	5.20
31	93.10	78.30	14.80	82.76	42.45	40.31	94.83	94.34	0.49
32	95.71	84.72	10.99	85.24	63.89	21.35	98.57	97.22	1.35
33	83.24	80.00	3.24	92.20	82.00	10.20	86.42	80.00	6.42
34	65.03	61.90	3.13	69.23	59.05	10.18	76.92	71.43	5.49
35	76.42	36.13	40.29	67.48	26.05	41.43	88.62	61.34	27.27
36	16.92	5.75	11.17	33.85	13.72	20.13	83.08	67.70	15.38
37	79.47	62.61	16.86	74.90	45.95	28.96	93.16	82.43	10.72
38	96.70	77.36	19.34	80.66	55.66	25.00	98.11	83.02	15.09
39	99.21	79.09	20.12	97.62	70.91	26.71	100.00	90.91	9.09
40	49.23	23.40	25.83	56.92	17.02	39.90	58.46	14.89	43.57
41	86.90	61.36	25.53	68.97	48.86	20.10	80.69	56.82	23.87
42	75.73	85.00	-9.27	84.47	67.00	17.47	90.29	93.00	-2.71
43	67.37	66.67	0.70	37.89	22.92	14.98	64.21	60.42	3.79
44	22.08	3.92	18.16	18.18	0.00	18.18	72.73	24.51	48.22
45	72.52	51.43	21.09	72.52	40.95	31.57	80.92	53.33	27.58

https://doi.org/10.52202/079017-3893

Table 22: Class-wise 1 vs. 1000 performance on `CounterAnimal` for `ViT-B/32` CLIP-trained on different datasets.

class ID	CLIP-LAION2B-ViT-B/32			CLIP-LAION400M-ViT-B/32			CLIP-OpenAI-ViT-B/32		
	easy	hard	drop	easy	hard	drop	easy	hard	drop
1	86.41	79.65	6.76	79.61	57.52	22.09	81.55	66.37	15.18
2	86.32	72.97	13.35	78.63	49.55	29.08	85.47	58.56	26.91
3	10.66	9.73	0.93	28.69	14.59	14.09	18.85	12.43	6.42
4	91.54	74.69	16.85	81.15	48.15	33.01	77.69	38.27	39.42
5	75.51	55.10	20.41	87.76	41.84	45.92	61.22	38.78	22.45
6	83.58	64.56	19.02	73.36	48.10	25.26	77.74	65.82	11.91
7	72.27	29.67	42.60	73.64	18.68	54.96	88.64	67.03	21.60
8	92.31	77.50	14.81	73.85	49.00	24.85	87.69	72.50	15.19
9	44.00	25.00	19.00	54.00	30.83	23.17	70.00	35.83	34.17
10	87.55	43.00	44.55	60.64	4.00	56.64	67.87	15.00	52.87
11	68.64	45.07	23.57	74.26	28.87	45.39	53.85	11.27	42.58
12	82.42	41.67	40.75	72.53	35.71	36.81	78.02	61.90	16.12
13	31.53	11.38	20.14	22.17	2.44	19.73	38.92	16.26	22.66
14	60.09	47.96	12.13	32.46	22.45	10.01	17.98	18.37	-0.38
15	71.79	22.89	48.90	67.95	19.68	48.27	75.64	31.33	44.32
16	71.52	15.95	55.57	68.87	1.23	67.65	72.85	8.59	64.26
17	61.08	36.00	25.08	48.50	20.00	28.50	54.29	32.80	21.49
18	67.09	39.77	27.41	29.11	4.17	24.95	74.68	25.76	48.93
19	68.40	60.76	7.64	81.82	43.67	38.15	77.49	51.27	26.22
20	73.77	54.81	18.96	55.74	20.19	35.55	70.49	34.62	35.88
21	69.23	31.82	37.41	73.08	43.94	29.14	67.31	27.27	40.03
22	92.98	62.62	30.37	96.49	67.29	29.20	89.47	53.27	36.20
23	64.86	37.93	26.93	59.85	17.24	42.60	60.62	32.18	28.43
24	95.09	71.00	24.09	88.34	63.00	25.34	95.09	85.00	10.09
25	91.67	57.55	34.12	93.63	68.87	24.76	96.57	83.96	12.61
26	13.60	0.45	13.15	20.00	4.07	15.93	15.20	0.45	14.75
27	66.67	48.32	18.34	77.78	14.77	63.01	77.78	69.13	8.65
28	68.53	49.50	19.02	79.70	55.45	24.25	63.45	16.83	46.62
29	85.37	53.77	31.59	80.49	39.62	40.87	78.54	46.23	32.31
30	93.10	61.62	31.49	86.21	71.72	14.49	82.76	30.30	52.46
31	86.21	63.21	23.00	82.76	42.45	40.31	91.38	68.87	22.51
32	95.71	84.72	10.99	85.24	63.89	21.35	88.57	72.22	16.35
33	85.84	80.00	5.84	92.20	82.00	10.20	76.59	80.00	-3.41
34	49.65	36.19	13.46	69.23	59.05	10.18	69.93	56.19	13.74
35	78.05	21.85	56.20	67.48	26.05	41.43	73.17	48.74	24.43
36	61.54	42.92	18.62	33.85	13.72	20.13	58.46	46.46	12.00
37	83.27	51.80	31.47	74.90	45.95	28.96	85.55	62.22	19.34
38	92.92	68.87	24.06	80.66	55.66	25.00	78.77	47.17	31.60
39	96.03	76.36	19.67	97.62	70.91	26.71	100.00	93.64	16.36
40	64.62	34.04	30.57	56.92	17.02	39.90	56.92	25.53	31.39
41	86.21	54.55	31.66	68.97	48.86	20.10	86.21	84.09	2.12
42	72.82	69.00	3.82	84.47	67.00	17.47	71.84	71.00	0.84
43	67.37	59.38	7.99	37.89	22.92	14.98	69.47	62.50	6.97
44	63.64	19.61	44.03	18.18	0.00	18.18	10.39	2.94	7.45
45	70.99	48.57	22.42	72.52	40.95	31.57	35.88	30.48	5.40

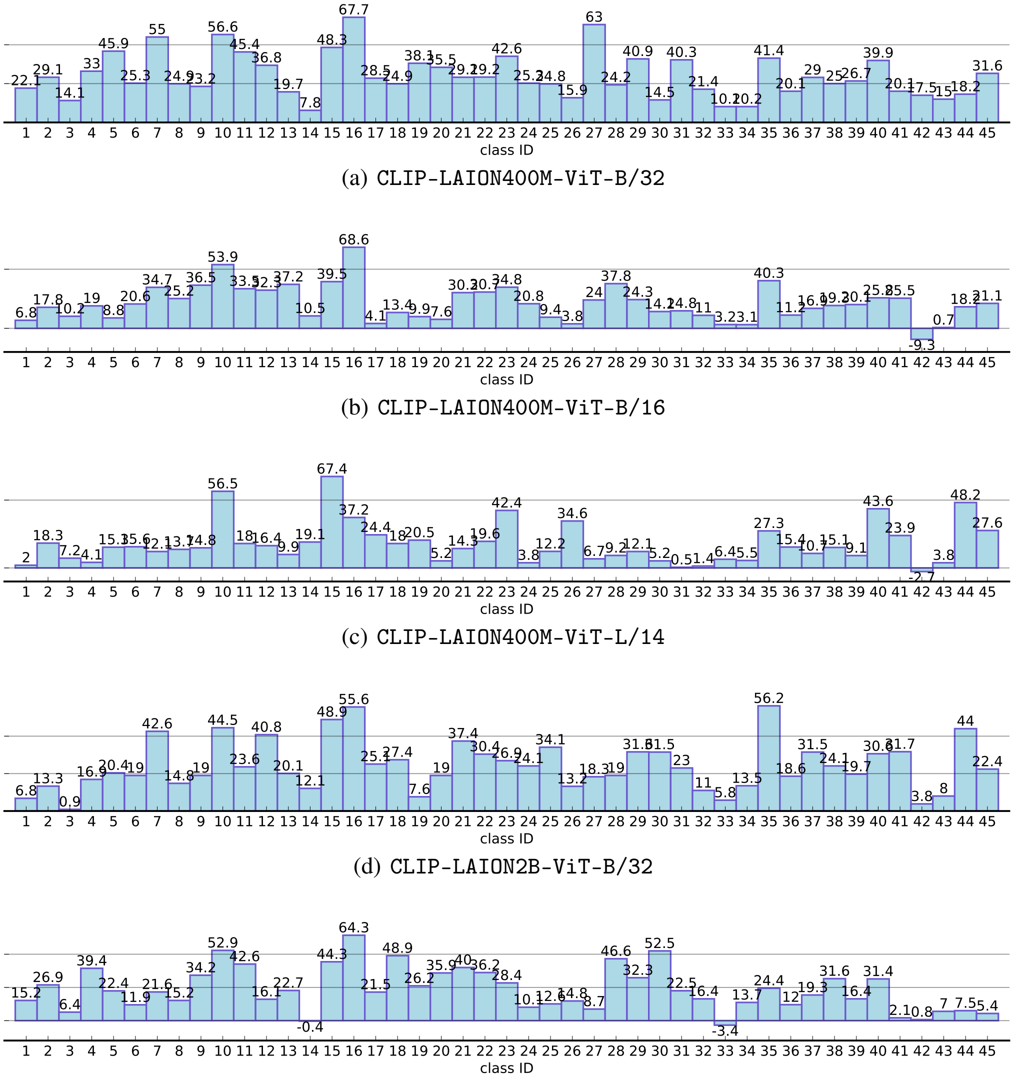

(a) CLIP-LAION400M-ViT-B/32

(b) CLIP-LAION400M-ViT-B/16

(c) CLIP-LAION400M-ViT-L/14

(d) CLIP-LAION2B-ViT-B/32

(e) CLIP-OpenAI-ViT-B/32

Figure 17: The performance drop (%) between easy to hard on varying CLIP setups. The horizontal axis denotes the class ids and the vertical axis denotes the class-wise accuracy drop.

NeurIPS Paper Checklist

1. **Claims**

   Question: Do the main claims made in the abstract and introduction accurately reflect the paper's contributions and scope?

   Answer: [Yes]

   Justification: Our main claim is that CLIP may not rely less on spurious features compared to ImageNet models. To support our claim, we curate a new evaluation dataset named `CounterAnimal`, specifically tailored for a comparative evaluation for the robustness of CLIP. Furthermore, we also conduct comprehensive experiments in Section 3 and theoretical justification in Section 4, both of which fully support our main position.

   Guidelines:

   - The answer NA means that the abstract and introduction do not include the claims made in the paper.
   - The abstract and/or introduction should clearly state the claims made, including the contributions made in the paper and important assumptions and limitations. A No or NA answer to this question will not be perceived well by the reviewers.
   - The claims made should match theoretical and experimental results, and reflect how much the results can be expected to generalize to other settings.
   - It is fine to include aspirational goals as motivation as long as it is clear that these goals are not attained by the paper.

2. **Limitations**

   Question: Does the paper discuss the limitations of the work performed by the authors?

   Answer: [Yes]

   Justification: We discuss the limitation of our work in Appendix A, especially focusing on the further improvements for our dataset.

   Guidelines:

   - The answer NA means that the paper has no limitation while the answer No means that the paper has limitations, but those are not discussed in the paper.
   - The authors are encouraged to create a separate "Limitations" section in their paper.
   - The paper should point out any strong assumptions and how robust the results are to violations of these assumptions (e.g., independence assumptions, noiseless settings, model well-specification, asymptotic approximations only holding locally). The authors should reflect on how these assumptions might be violated in practice and what the implications would be.
   - The authors should reflect on the scope of the claims made, e.g., if the approach was only tested on a few datasets or with a few runs. In general, empirical results often depend on implicit assumptions, which should be articulated.
   - The authors should reflect on the factors that influence the performance of the approach. For example, a facial recognition algorithm may perform poorly when image resolution is low or images are taken in low lighting. Or a speech-to-text system might not be used reliably to provide closed captions for online lectures because it fails to handle technical jargon.
   - The authors should discuss the computational efficiency of the proposed algorithms and how they scale with dataset size.
   - If applicable, the authors should discuss possible limitations of their approach to address problems of privacy and fairness.
   - While the authors might fear that complete honesty about limitations might be used by reviewers as grounds for rejection, a worse outcome might be that reviewers discover limitations that aren't acknowledged in the paper. The authors should use their best judgment and recognize that individual actions in favor of transparency play an important role in developing norms that preserve the integrity of the community. Reviewers will be specifically instructed to not penalize honesty concerning limitations.

3. **Theory Assumptions and Proofs**

https://doi.org/10.52202/079017-3893

Question: For each theoretical result, does the paper provide the full set of assumptions and a complete (and correct) proof?

Answer: [Yes]

Justification: In Definition 1, we clearly outline the assumptions made for the subsequent theoretical analysis presented in Theorem 1. In Appendix D, we present further details regarding our assumptions, proofs, and the associated experiments to validate their feasibility.

Guidelines:

- The answer NA means that the paper does not include theoretical results.
- All the theorems, formulas, and proofs in the paper should be numbered and cross-referenced.
- All assumptions should be clearly stated or referenced in the statement of any theorems.
- The proofs can either appear in the main paper or the supplemental material, but if they appear in the supplemental material, the authors are encouraged to provide a short proof sketch to provide intuition.
- Inversely, any informal proof provided in the core of the paper should be complemented by formal proofs provided in appendix or supplemental material.
- Theorems and Lemmas that the proof relies upon should be properly referenced.

4. **Experimental Result Reproducibility**

Question: Does the paper fully disclose all the information needed to reproduce the main experimental results of the paper to the extent that it affects the main claims and/or conclusions of the paper (regardless of whether the code and data are provided or not)?

Answer: [Yes]

Justification: In Section 2.1, we elaborate on the exact process used to construct the `CounterAnimal` dataset, including details about the raw data sources, the construction pipeline, and the dataset configurations. Moreover, for reproducibility, most of our experiments utilize open-sourced model checkpoints from the OpenCLIP and PyTorch repositories. We also comprehensively document the evaluation setups in Appendix C. We will release our dataset and the evaluation codes in the future.

Guidelines:

- The answer NA means that the paper does not include experiments.
- If the paper includes experiments, a No answer to this question will not be perceived well by the reviewers: Making the paper reproducible is important, regardless of whether the code and data are provided or not.
- If the contribution is a dataset and/or model, the authors should describe the steps taken to make their results reproducible or verifiable.
- Depending on the contribution, reproducibility can be accomplished in various ways. For example, if the contribution is a novel architecture, describing the architecture fully might suffice, or if the contribution is a specific model and empirical evaluation, it may be necessary to either make it possible for others to replicate the model with the same dataset, or provide access to the model. In general. releasing code and data is often one good way to accomplish this, but reproducibility can also be provided via detailed instructions for how to replicate the results, access to a hosted model (e.g., in the case of a large language model), releasing of a model checkpoint, or other means that are appropriate to the research performed.
- While NeurIPS does not require releasing code, the conference does require all submissions to provide some reasonable avenue for reproducibility, which may depend on the nature of the contribution. For example
  (a) If the contribution is primarily a new algorithm, the paper should make it clear how to reproduce that algorithm.
  (b) If the contribution is primarily a new model architecture, the paper should describe the architecture clearly and fully.
  (c) If the contribution is a new model (e.g., a large language model), then there should either be a way to access this model for reproducing the results or a way to reproduce the model (e.g., with an open-source dataset or instructions for how to construct the dataset).

https://doi.org/10.52202/079017-3893

(d) We recognize that reproducibility may be tricky in some cases, in which case authors are welcome to describe the particular way they provide for reproducibility. In the case of closed-source models, it may be that access to the model is limited in some way (e.g., to registered users), but it should be possible for other researchers to have some path to reproducing or verifying the results.

5. **Open access to data and code**

   Question: Does the paper provide open access to the data and code, with sufficient instructions to faithfully reproduce the main experimental results, as described in supplemental material?

   Answer: [Yes]

   Justification: We establish an anonymous repository for the access to our dataset, which can be found at the link of `https://figshare.com/s/f9b0f34312168f4a8ddb`. We will provide clearer and easier access instructions once the paper is accepted.

   Guidelines:

   - The answer NA means that paper does not include experiments requiring code.
   - Please see the NeurIPS code and data submission guidelines (`https://nips.cc/public/guides/CodeSubmissionPolicy`) for more details.
   - While we encourage the release of code and data, we understand that this might not be possible, so "No" is an acceptable answer. Papers cannot be rejected simply for not including code, unless this is central to the contribution (e.g., for a new open-source benchmark).
   - The instructions should contain the exact command and environment needed to run to reproduce the results. See the NeurIPS code and data submission guidelines (`https://nips.cc/public/guides/CodeSubmissionPolicy`) for more details.
   - The authors should provide instructions on data access and preparation, including how to access the raw data, preprocessed data, intermediate data, and generated data, etc.
   - The authors should provide scripts to reproduce all experimental results for the new proposed method and baselines. If only a subset of experiments are reproducible, they should state which ones are omitted from the script and why.
   - At submission time, to preserve anonymity, the authors should release anonymized versions (if applicable).
   - Providing as much information as possible in supplemental material (appended to the paper) is recommended, but including URLs to data and code is permitted.

6. **Experimental Setting/Details**

   Question: Does the paper specify all the training and test details (e.g., data splits, hyperparameters, how they were chosen, type of optimizer, etc.) necessary to understand the results?

   Answer: [Yes]

   Justification: We utilize open-sourced model checkpoints from OpenCLIP and PyTorch. We collect the `CounterAnimal` dataset following the precise pipelines in Section 2.1. Moreover, we detail the evaluation setups of our experiments in Appendix C.

   We utilize open-sourced model checkpoints from OpenCLIP and PyTorch; we have collected the `CounterAnimal` dataset according to the procedures outlined in Section 2.1; and we provide detailed descriptions of our evaluation setups in Appendix C.

   Guidelines:

   - The answer NA means that the paper does not include experiments.
   - The experimental setting should be presented in the core of the paper to a level of detail that is necessary to appreciate the results and make sense of them.
   - The full details can be provided either with the code, in appendix, or as supplemental material.

7. **Experiment Statistical Significance**

   Question: Does the paper report error bars suitably and correctly defined or other appropriate information about the statistical significance of the experiments?

Answer: [No]

Justification: We utilize open-sourced model checkpoints without additional training or fine-tuning, and employ the complete dataset of `CounterAnimal` to conduct our experiments. There is no stochastic factor that may appear in our experiments, and thus we do not need to report the error bars for our results.

Guidelines:

- The answer NA means that the paper does not include experiments.
- The authors should answer "Yes" if the results are accompanied by error bars, confidence intervals, or statistical significance tests, at least for the experiments that support the main claims of the paper.
- The factors of variability that the error bars are capturing should be clearly stated (for example, train/test split, initialization, random drawing of some parameter, or overall run with given experimental conditions).
- The method for calculating the error bars should be explained (closed form formula, call to a library function, bootstrap, etc.)
- The assumptions made should be given (e.g., Normally distributed errors).
- It should be clear whether the error bar is the standard deviation or the standard error of the mean.
- It is OK to report 1-sigma error bars, but one should state it. The authors should preferably report a 2-sigma error bar than state that they have a 96% CI, if the hypothesis of Normality of errors is not verified.
- For asymmetric distributions, the authors should be careful not to show in tables or figures symmetric error bars that would yield results that are out of range (e.g. negative error rates).
- If error bars are reported in tables or plots, The authors should explain in the text how they were calculated and reference the corresponding figures or tables in the text.

8. **Experiments Compute Resources**

   Question: For each experiment, does the paper provide sufficient information on the computer resources (type of compute workers, memory, time of execution) needed to reproduce the experiments?

   Answer: [Yes]

   Justification: We provide details our hardware configurations in Appendix C.1. However, we do not list memory and time requirements since our experiments are not computationally demanding.

   Guidelines:

   - The answer NA means that the paper does not include experiments.
   - The paper should indicate the type of compute workers CPU or GPU, internal cluster, or cloud provider, including relevant memory and storage.
   - The paper should provide the amount of compute required for each of the individual experimental runs as well as estimate the total compute.
   - The paper should disclose whether the full research project required more compute than the experiments reported in the paper (e.g., preliminary or failed experiments that didn't make it into the paper).

9. **Code Of Ethics**

   Question: Does the research conducted in the paper conform, in every respect, with the NeurIPS Code of Ethics `https://neurips.cc/public/EthicsGuidelines`?

   Answer: [Yes]

   Justification: Our research conform with the NeurIPS Code of Ethics.

   Guidelines:

   - The answer NA means that the authors have not reviewed the NeurIPS Code of Ethics.
   - If the authors answer No, they should explain the special circumstances that require a deviation from the Code of Ethics.

https://doi.org/10.52202/079017-3893

- The authors should make sure to preserve anonymity (e.g., if there is a special consideration due to laws or regulations in their jurisdiction).

10. **Broader Impacts**

    Question: Does the paper discuss both potential positive societal impacts and negative societal impacts of the work performed?

    Answer: [Yes]

    Justification: We discuss the broader impacts of our work in Appendix A, focusing on our impacts for both the research community and the real-world applications.

    Guidelines:

    - The answer NA means that there is no societal impact of the work performed.
    - If the authors answer NA or No, they should explain why their work has no societal impact or why the paper does not address societal impact.
    - Examples of negative societal impacts include potential malicious or unintended uses (e.g., disinformation, generating fake profiles, surveillance), fairness considerations (e.g., deployment of technologies that could make decisions that unfairly impact specific groups), privacy considerations, and security considerations.
    - The conference expects that many papers will be foundational research and not tied to particular applications, let alone deployments. However, if there is a direct path to any negative applications, the authors should point it out. For example, it is legitimate to point out that an improvement in the quality of generative models could be used to generate deepfakes for disinformation. On the other hand, it is not needed to point out that a generic algorithm for optimizing neural networks could enable people to train models that generate Deepfakes faster.
    - The authors should consider possible harms that could arise when the technology is being used as intended and functioning correctly, harms that could arise when the technology is being used as intended but gives incorrect results, and harms following from (intentional or unintentional) misuse of the technology.
    - If there are negative societal impacts, the authors could also discuss possible mitigation strategies (e.g., gated release of models, providing defenses in addition to attacks, mechanisms for monitoring misuse, mechanisms to monitor how a system learns from feedback over time, improving the efficiency and accessibility of ML).

11. **Safeguards**

    Question: Does the paper describe safeguards that have been put in place for responsible release of data or models that have a high risk for misuse (e.g., pre-trained language models, image generators, or scraped datasets)?

    Answer: [Yes]

    Justification: To avoid any safety risk, we control the label space for our `CounterAnimal` dataset and manually cleanse any unsafe image during our data collection procedure.

    Guidelines:

    - The answer NA means that the paper poses no such risks.
    - Released models that have a high risk for misuse or dual-use should be released with necessary safeguards to allow for controlled use of the model, for example by requiring that users adhere to usage guidelines or restrictions to access the model or implementing safety filters.
    - Datasets that have been scraped from the Internet could pose safety risks. The authors should describe how they avoided releasing unsafe images.
    - We recognize that providing effective safeguards is challenging, and many papers do not require this, but we encourage authors to take this into account and make a best faith effort.

12. **Licenses for existing assets**

    Question: Are the creators or original owners of assets (e.g., code, data, models), used in the paper, properly credited and are the license and terms of use explicitly mentioned and properly respected?

https://doi.org/10.52202/079017-3893

Answer: [Yes]

Justification: For models, only open-sourced checkpoints are adopted, following the licenses from https://github.com/mlfoundations/open_clip/blob/main/LICENSE and https://github.com/pytorch/pytorch/blob/main/LICENSE. The versions of the adopted OpenCLIP checkpoints can be found in Table 6. For scraped data, we only use those photos from iNaturalist following the CC BY-NC license, which are allowed for scientific usage. Please refer to the following link for the details about CC BY-NC: https://creativecommons.org/licenses/by-nc/4.0/.

Guidelines:

- The answer NA means that the paper does not use existing assets.
- The authors should cite the original paper that produced the code package or dataset.
- The authors should state which version of the asset is used and, if possible, include a URL.
- The name of the license (e.g., CC-BY 4.0) should be included for each asset.
- For scraped data from a particular source (e.g., website), the copyright and terms of service of that source should be provided.
- If assets are released, the license, copyright information, and terms of use in the package should be provided. For popular datasets, paperswithcode.com/datasets has curated licenses for some datasets. Their licensing guide can help determine the license of a dataset.
- For existing datasets that are re-packaged, both the original license and the license of the derived asset (if it has changed) should be provided.
- If this information is not available online, the authors are encouraged to reach out to the asset's creators.

13. **New Assets**

Question: Are new assets introduced in the paper well documented and is the documentation provided alongside the assets?

Answer: [Yes]

Justification: Our CounterAnimal dataset follows the MIT license. Permission is hereby granted, free of charge, to any person obtaining a copy of this software and associated documentation files, to deal in the Software without restriction, including without limitation the rights to use, copy, modify, merge, publish, distribute, sublicense, and/or sell copies of the Software, and to permit persons to whom the Software is furnished to do so, subject to the following conditions: The above copyright notice and this permission notice shall be included in all copies or substantial portions of the Software.

Guidelines:

- The answer NA means that the paper does not release new assets.
- Researchers should communicate the details of the dataset/code/model as part of their submissions via structured templates. This includes details about training, license, limitations, etc.
- The paper should discuss whether and how consent was obtained from people whose asset is used.
- At submission time, remember to anonymize your assets (if applicable). You can either create an anonymized URL or include an anonymized zip file.

14. **Crowdsourcing and Research with Human Subjects**

Question: For crowdsourcing experiments and research with human subjects, does the paper include the full text of instructions given to participants and screenshots, if applicable, as well as details about compensation (if any)?

Answer: [Yes]

Justification: The CounterAnimal dataset is constructed with human labeling, yet without crowdsourcing. The labeling and filtering procedure adhere strictly to the pipeline outlined in Section 2.1. Our project does not involve any form of compensation or profit. All individuals involved in the manual data curation are from our team, and they all have been notified and agreed to grant consent to the use of the data in this work. this work.

https://doi.org/10.52202/079017-3893

- The answer NA means that the paper does not involve crowdsourcing nor research with human subjects.
- Including this information in the supplemental material is fine, but if the main contribution of the paper involves human subjects, then as much detail as possible should be included in the main paper.
- According to the NeurIPS Code of Ethics, workers involved in data collection, curation, or other labor should be paid at least the minimum wage in the country of the data collector.

15. **Institutional Review Board (IRB) Approvals or Equivalent for Research with Human Subjects**

    Question: Does the paper describe potential risks incurred by study participants, whether such risks were disclosed to the subjects, and whether Institutional Review Board (IRB) approvals (or an equivalent approval/review based on the requirements of your country or institution) were obtained?

    Answer: [NA]

    Justification: [NA]

    Guidelines:

    - The answer NA means that the paper does not involve crowdsourcing nor research with human subjects.
    - Depending on the country in which research is conducted, IRB approval (or equivalent) may be required for any human subjects research. If you obtained IRB approval, you should clearly state this in the paper.
    - We recognize that the procedures for this may vary significantly between institutions and locations, and we expect authors to adhere to the NeurIPS Code of Ethics and the guidelines for their institution.
    - For initial submissions, do not include any information that would break anonymity (if applicable), such as the institution conducting the review.

https://doi.org/10.52202/079017-3893